

GAN KAI HAN

B. ENG. (HONS) CIVIL ENGINEERING

JANUARY 2016

WAVE TRANSMISSION CHARACTERISTICS OF THE  
RAPIDLY INSTALLED MODULAR FLOATING  
BREAKWATER

**GAN KAI HAN**

CIVIL ENGINEERING  
UNIVERSITI TEKNOLOGI PETRONAS  
JANUARY 2016

# **Wave Transmission Characteristics of the Rapidly Installed Modular Floating Breakwaters**

By

Gan Kai Han

16284

Dissertation submitted in partial fulfilment  
of the requirements for the  
Bachelor of Engineering (Hons)  
(Civil)

JANUARY 2016

Universiti Teknologi PETRONAS  
Bandar Seri Iskandar  
31750 Tronoh  
Perak Darul Ridzuan

# CERTIFICATION OF APPROVAL

## **Wave Transmission Characteristics of the Rapidly Installed Modular Floating Breakwaters**

By

Gan Kai Han

16284

Dissertation submitted to the  
Civil Engineering Department  
of Universiti Teknologi PETRONAS  
in partial fulfillment of the requirement for the  
BACHELOR OF ENGINEERING (Hons)  
(CIVIL)

Approved by,

---

(Dr. Teh Hee Min)

UNIVERSITI TEKNOLOGI PETRONAS  
TRONOH, PERAK

January 2016

# CERTIFICATION OF ORIGINALITY

This is to certify that I am responsible for the work submitted in this project, that the original work is my own except as specified in the references and acknowledgements, and that the original work contained herein have not been undertaken or done by unspecified sources or persons.

---

Gan Kai Han

## **Abstract**

Many military and naval operations have required some kind of wave attenuating system that can be installed rapidly for the operations to be carried out smoothly and be uninstalled when the operations have finished. This has led to the need to develop a more flexible floating breakwater which can serve the purpose. Thus, modular floating breakwaters with Lego-based design have been proposed due to their rapid installation characteristic. This research study aimed to study the wave transmission characteristics of the rapidly installed modular floating breakwaters in regular waves. The two main objectives in this study were to evaluate the effects of breakwater width and draft on wave transmission characteristics of the rapidly installed modular floating breakwaters and also to compare wave attenuation performance of the rapidly installed modular floating breakwaters of different irregular configurations. This study was a physical modelling-based project which had 19 breakwater models with a total number of 171 test runs. Each model was tested against 3 different wave periods (0.8s, 1.2s and 1.6s) and 3 different stroke adjustments (40mm, 120mm and 200mm) that produced incident wave heights ranging from 1cm to 6.5cm at a constant water depth of 0.3m. The wave attenuation performance of modular floating breakwaters were evaluated and analyzed based on wave transmission coefficient,  $C_t$  value.

# **Table of Content**

<b>Certification of Approval</b>	ii
<b>Certification of Originality</b>	iii
<b>Abstract</b>	iv
<b>List of Tables</b>	vii
<b>List of Figures</b>	viii
<b>Chapter 1: Introduction</b>	1
1.1 General	1
1.2 Background of study	1
1.3 Problem Statement	3
1.4 Objectives	3
1.5 Significance of study	4
1.6 Scope of study	4
<b>Chapter 2: Literature Review</b>	5
2.1 General	5
2.2 Waves interactions	5
2.2.1 Wave transmission	5
2.2.2 Wave reflection	6
2.2.3 Energy loss	6
2.3 Existing Types of Floating Breakwaters	8
2.4 Scaling Laws for Scale Effects	17
2.4.1 Froude Number	17
2.4.2 Reynolds Number	18
2.4.3 Weber Number	19
<b>Chapter 3: Methodology</b>	20
3.1 General	20
3.2 Physical Models	20

3.3 Laboratory Equipment and Instrument	23
3.3.1 Wave flume	23
3.3.2 Wave paddle	23
3.3.3 Wave absorber	24
3.4 Experimental Set-up	26
i) Effect of breakwater width and height	26
ii) Effect of different breakwater configurations	27
3.5 Flow Chart	31
3.6 Gantt Chart	32
3.7 Key Milestones	32
<b>Chapter 4: Results and Discussion</b>	<b>34</b>
4.1 General	34
4.2 Effect of wave steepness	35
4.2.1 Effect of breakwater width and height	35
4.2.1.1 Summary	41
4.2.2 Effect of different breakwater configurations	42
4.3 Effect of relative width	48
4.3.1 Effect of breakwater width and height	48
4.2.1.1 Summary	56
4.3.2 Effect of different breakwater configurations	57
<b>Chapter 5: Conclusion and Recommendations</b>	<b>61</b>
5.1 Conclusion	61
5.2 Recommendations	62
<b>References</b>	<b>63</b>

## **List of Tables**

Table 3.1:	Arrangements of physical models to evaluate the effects of breakwater width and draft on wave transmission characteristics of the rapidly installed modular floating breakwaters	26
Table 3.2:	Arrangements of physical models to compare wave attenuation of the rapidly installed modular floating breakwaters of different irregular configurations	27
Table 3.3:	Parameters used in the experiment	29
Table 3.4:	Wave condition at water depth of 30cm	30
Table 3.5:	Gantt Chart	32
Table 3.6:	Key milestone for FYP 1	32
Table 3.7:	Key milestone for FYP 2	33
Table 4.1:	Test parameters for single layer models	36
Table 4.2:	Statistics of $C_t$ values for single layer models	36
Table 4.3:	Test parameters for double layer models	38
Table 4.4:	Statistics of $C_t$ values for double layer models	38
Table 4.5:	Test parameters for triple layer models	40
Table 4.6:	Statistics of $C_t$ values for triple layer models	40
Table 4.7:	Test parameters for 2 x 2 matrix models	43
Table 4.8:	Statistics of $C_t$ values for 2 x 2 matrix models	43
Table 4.9:	Test parameters for 2 x 3 matrix models	46
Table 4.10:	Statistics of $C_t$ values for 2 x 3 matrix models	46
Table 4.11:	Test parameters for single column models	49
Table 4.12:	Test parameters for double column models	51
Table 4.13:	Test parameters for triple column models	53
Table 4.14:	Test parameters for quadruple column models	55
Table 4.15:	Test parameters for 2 x 2 matrix models	58
Table 4.16:	Test parameters for 2 x 3 matrix models	60

## **List of Figures**

Figure 1.1:	Types of breakwaters available	2
Figure 2.1:	Mooring line configurations for single pontoon floating	8
Figure 2.2:	Dual pontoon breakwater sketch	9
Figure 2.3:	Pneumatic floating breakwater and original rectangular breakwater	10
Figure 2.4:	Schematic diagram of $\pi$ shaped floating breakwater	10
Figure 2.5:	Details of Y-framed floating breakwater	11
Figure 2.6:	Board-net floating breakwater	12
Figure 2.7:	H shaped floating breakwater	12
Figure 2.8:	3D sketch of Cylindrical Floating Breakwater	13
Figure 2.9:	Rapidly Installed Breakwater (RIB) System developed by U.S. Army	14
Figure 2.10:	Change between the incident wave energy and the transmitted wave energy of XM 2000 RIB	15
Figure 2.11:	WaveEater	15
Figure 2.12:	WhisprWave®	16
Figure 2.13:	Wavebrake	16
Figure 3.1:	Rectangular-shaped module	20
Figure 3.2:	Front view of rectangular-shaped module	20
Figure 3.3:	Right side view of rectangular-shaped module	21
Figure 3.4:	Triangular-shaped module	21
Figure 3.5:	Front view of triangular-shaped module	21
Figure 3.6:	Right side view of triangular-shaped module	22
Figure 3.7:	Brass stop pipe plus	22
Figure 3.8:	Wave flume	23
Figure 3.9:	Wave paddle	24
Figure 3.10:	Wave absorber	25
Figure 3.11:	Wave absorber (side view)	25
Figure 3.12:	Experimental set-up (plan view)	28
Figure 3.13:	Experiment set-up (side view)	28
Figure 3.14:	Procedures conducted	31

Figure 4.1:	Effect of breakwater width on $C_t$ of the single layer models ( $D/d = 0.167$ )	35
Figure 4.2:	Effect of breakwater width on $C_t$ of the double layer models ( $D/d = 0.333$ )	37
Figure 4.3:	Effect of breakwater width on $C_t$ of the triple layer models ( $D/d = 0.667$ )	39
Figure 4.4:	Effect of breakwater configuration on $C_t$ of the 2 x 2 matrix models ( $D/d = 0.333$ )	42
Figure 4.5:	Effect of breakwater configuration on $C_t$ of the 2 x 3 matrix models ( $D/d = 0.333$ )	45
Figure 4.6:	Effect of breakwater draft on $C_t$ of the single column models ( $B/d = 0.333$ )	48
Figure 4.7:	Effect of breakwater draft on $C_t$ of the double column models ( $B/d = 0.667$ )	50
Figure 4.8:	Effect of breakwater draft on $C_t$ of the triple column models ( $B/d = 1.000$ )	52
Figure 4.9:	Effect of breakwater draft on $C_t$ of the quadruple column models ( $B/d = 1.333$ )	54
Figure 4.10:	Effect of breakwater draft on $C_t$ of the 2 x 2 matrix models ( $B/d = 0.667$ )	57
Figure 4.11:	Effect of breakwater draft on $C_t$ of the 2 x 3 matrix models ( $B/d = 1.000$ )	59

# **CHAPTER 1**

## **INTRODUCTION**

### **1.1 GENERAL**

This chapter will introduce background of floating breakwater and the problems associated with it. Besides that, objectives, significance and scope of this research will also be included in this chapter.

### **1.2 BACKGROUND OF STUDY**

Breakwaters are common coastal engineering structures that are built near the coastlines to serve as a protection for harbors and the shore as well. They have the capability of attenuating incident waves and creating a calm basin at the leeward side of the structure. The most conventional type of breakwaters are the bottom-mounted breakwaters. They offer excellent storm protection and have high durability in withstanding destructive waves. Despite of that, they are not economic and environmental-friendly. The cost of construction of the bottom-fixed breakwaters will increase exponentially with the water depth (Kumar, 2008). According to McCartney (1985), in area which has water depth more than 20ft, it is often more expensive to construct bottom-mounted breakwaters than floating breakwaters. Moreover, these structures have longer construction period and the quality of water will be affected during construction (Dillon Consulting Limited, 2013). Furthermore, they cannot be removed once constructed at site.

Due to the limitations of the fixed breakwaters, researchers developed various types of floating breakwaters over the past decades to serve as an alternative to the conventional bottom-mounted breakwaters. Wave attenuation of floating breakwaters might not be as good as the fixed breakwaters. However they have the advantage of being able to be installed and removed easily. The layout can be easily changed to accommodate seasonal wave climate changes. Besides that, floating breakwaters have low construction cost as they are insensitive to the water depth. Therefore, floating breakwaters seem to be more preferable than the fixed structures in certain coastal engineering applications.

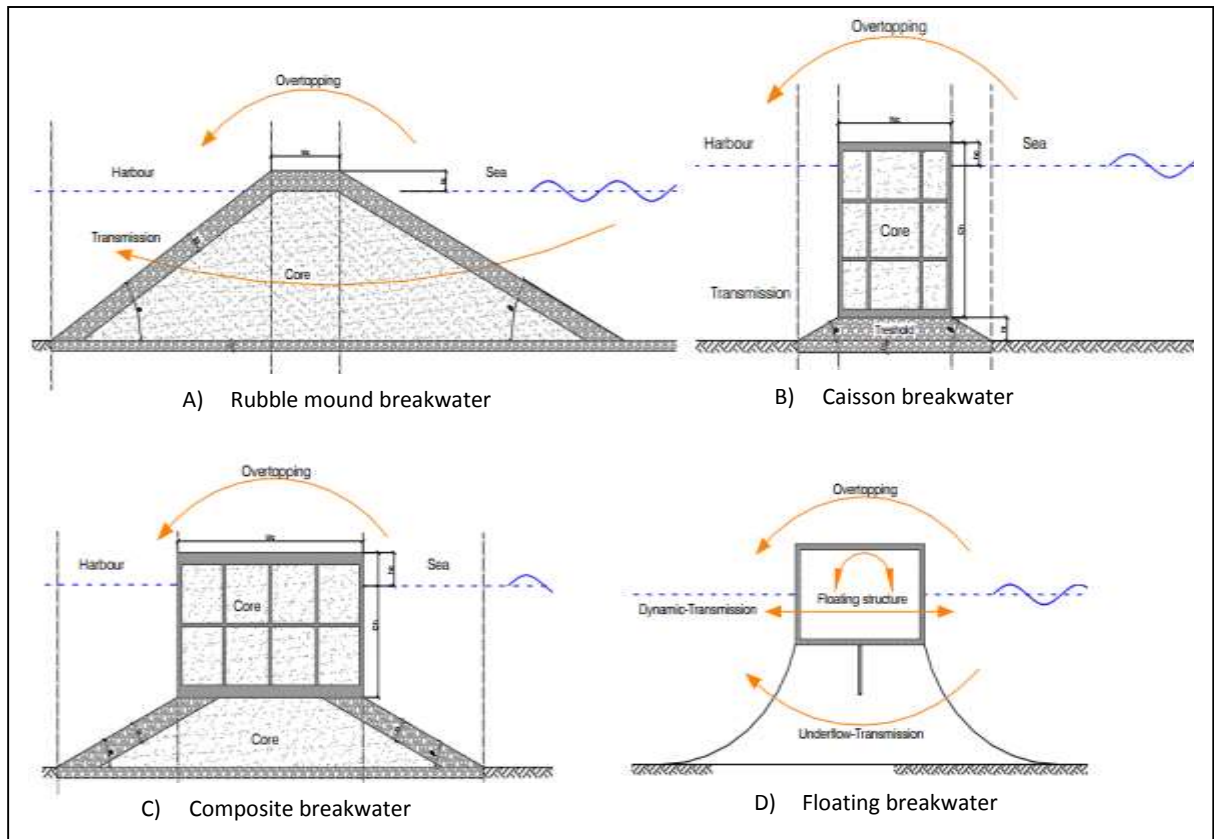


Figure 1.1: Types of breakwaters available (Fousert, 2006)

The advantages of floating breakwaters are as follows:

1. The construction cost of floating breakwaters does not increase exponentially with water depth.
2. Floating breakwaters can be reused and relocated.
3. Floating breakwaters will not impede the water circulation underneath the structure and fish migration.
4. Floating breakwaters are more aesthetically pleasing.

However, floating breakwaters have their own disadvantages as well. The disadvantages are as follows:

1. The design must be carefully matched to the site conditions.
2. Less effective in heavy storms and large period waves.
3. May cause damages if the mooring lines or anchors fail.

### **1.3 PROBLEM STATEMENT**

In recent years, many new designs of floating breakwaters have been developed. They have started to become more significant due to their benefits in terms of environmental and visual impact (Mulvihill et al., 1980). However, most of them are not being able to be installed rapidly at the site location. This is because they are mostly made up of multiparts, causing the installation works to be laborious and time consuming. The feature of being able to be installed rapidly is crucial for some military and naval operations, such as the “change of pilot” operation at the Kertih Port which require a temporal offshore perimeter shelter to be erected instantly for the operations to be carried out. Other than that, the existing floating breakwaters are also having logistics and transportation problems. Most of them are big and bulky, causing the transportation, loading and unloading works to be difficult. Besides that, the configurations of the existing floating barriers are fixed, causing the structure to be less versatile in responding to the sea wave action. To achieve the optimal performance, the configurations of floating breakwater should be able to change according to the sea and site conditions. These problems have led to the need of developing a more flexible floating breakwater.

### **1.4 OBJECTIVES**

The aim of this research was to determine wave transmission characteristics of the rapidly installed modular floating breakwaters in regular waves. This was accomplished by achieving the following objectives:

- To evaluate the effects of breakwater width and draft on wave transmission characteristics of the rapidly installed modular floating breakwaters.
- To compare wave attenuation performance of the rapidly installed modular floating breakwaters of different irregular configurations.

## **1.5 SIGNIFICANCE OF STUDY**

This modular floating breakwater was designed in such a way that it can be installed rapidly to provide a temporal offshore harbor for military and naval purposes. This novel floating breakwater can solve the problem faced by the U.S. Army and the pilots in Kertih Port during their operations at offshore area. Besides that, it can protect the coastal area from unpredictable monsoonal waves due to the change in climate. The feature of being able to be installed instantly can prevent the destructive waves from reaching to the shoreline and cause erosion. This amazing feature was due to the air-inflation technique and its Lego-based design. The modules can be connected to form different configurations hence accommodating a wider range of breakwater designs. Furthermore, it can also serve as a temporary breakwater during the installation of the permanent breakwaters. This will allow the installation works to be relatively easier since the waves have already been attenuated. In addition to that, the benefits of being able to be deployed easily and stored conveniently have made the modular floating breakwater extremely useful in rescue operations for aircraft crashes and vessel recovery operations.

## **1.6 SCOPE OF STUDY**

This research study had its own scopes and limitations. One of the scopes of this study was that only physical modeling is being considered. Numerical simulation was not being done due to the time constraint. Besides that, the tests were being carried out under regular head-on waves generated by the wave paddle, irregular and oblique waves were not being taken into considerations. In addition to that, the water depth in the wave flume for the tests was being fixed at 30cm. Furthermore, the test models were being subjected to a condition where there was wave only, no underwater current was present. Moreover, motion responses and the effect of mooring lines were not being taken into the scope of this research study. Last but not least, this research study used Froude modelling as the scaling law for scaling effects. It was believed that Froude scaling law provides the closest similitude between the model and prototype since the predominant force in the tests was the gravitational force.

## CHAPTER 2

### LITERATURE REVIEW

#### 2.1 GENERAL

This chapter will describe some of the common wave interactions of a floating breakwater. Besides that, the state-of-the-art designs of floating breakwaters and the scaling laws for scale effects will be discussed in this chapter as well.

#### 2.2 WAVE INTERACTIONS

When the propagation of waves is being disturbed by an obstacle like breakwater, the waves may experience a few forms of interactions depending on the characteristics of the obstacle. The wave interactions that this study will consider are wave transmission, wave reflection and wave dissipation.

##### 2.2.1 Wave Transmission

According to Chakrabarti (1999), the effectiveness of a breakwater can be measured by the amount of wave energy transmitted beyond the structure. Wave transmission coefficient can be calculated by using the following formula:

$$C_t = \frac{H_t}{H_i} \quad (2.1)$$

where,

$C_t$  is the transmission coefficient, ranging from 0 to 1

$H_t$  is the transmitted wave height

$H_i$  is the incident wave height

In order to be considered as effective, the transmission coefficient of a breakwater must be small (approaching 0). This shows that the energy that has been transmitted past the structure is less than the energy of the incident wave. A high transmission coefficient (approaching 1) means that the structure failed to attenuate the incoming wave energy.

### 2.2.2 Wave Reflection

When water waves strike a structure when propagating forward, some of the waves will “bounce back” from the structure. Chakrabarti (1999) described wave reflection as the redirection of non-dissipated wave energy by the shoreline or coastal structures to the sea. Wave reflection coefficient can be calculated by using the following formula:

$$C_r = \frac{H_r}{H_i} \quad (2.2)$$

where,

$C_r$  is the reflection coefficient, ranging from 0 to 1

$H_r$  is the reflected wave height

$H_i$  is the incident wave height

If  $C_r$  equals to 1, it means that the water waves are being reflected back to the sea completely. On the contrary, when  $C_r$  equals to 0, it simply means that no waves are being reflected at all. Hence if  $C_r$  is between 0 to 1, the waves are being partially reflected.

### 2.2.3 Wave Dissipation (Energy Loss)

Wave energy breaks down into a few components once the wave hits an obstacle or structure. The first component is the wave that is being reflected back seaward by the structure (reflected waves) and the second component is the wave that managed to pass through the structure (transmitted waves). The remaining component is the energy loss due to wave dissipation. The amount of energy loss or energy loss coefficient for a typical flow can be calculated using the following formula:

$$E_i = E_r + E_t + E_l \quad (2.3)$$

where,

$E_i$  is the incident wave energy

$E_r$  is the reflected wave energy

$E_t$  is the transmitted wave energy

$E_l$  is the energy loss

Wave Energy can be written in terms of wave height:

$$E = \frac{(\rho g H)^2}{8} \quad (2.4)$$

Substituting Eq. (2.4) into Eq. (2.3):

$$\frac{(\rho g H_i)^2}{8} = \frac{(\rho g H_r)^2}{8} + \frac{(\rho g H_t)^2}{8} + \frac{(\rho g H_l)^2}{8} \quad (2.5)$$

After the simplification, Eq. (2.5) becomes:

$$H_i^2 = H_r^2 + H_t^2 + H_l^2 \quad (2.6)$$

Dividing Eq. (2.6) by  $H_i^2$ :

$$1 = C_r^2 + C_t^2 + C_l^2 \quad (2.7)$$

where,

$C_r$  is the reflection coefficient

$C_t$  is the transmission coefficient

$C_l$  is the energy loss coefficient

By rearranging Eq. (2.7), energy loss coefficient is:

$$C_l^2 = 1 - C_r^2 - C_t^2 \quad (2.8)$$

## 2.3 EXISTING FLOATING BREAKWATERS

Over the years, many floating breakwaters have been developed by different researchers due to their benefits in terms of environmental and visual impact. The study of advantages and disadvantages of different types of floating breakwaters has been carried out by researchers like McCartney (1985) and Mani (1991). According to Hales (1981), the design of floating breakwaters should be kept as simple, durable and maintenance free as possible. Any highly complex structures that are difficult and expensive to design, construct and maintain should be avoided. Several existing types of floating breakwater that have been developed and tested will be discussed below.

The most common type of floating breakwater is the **single pontoon floating breakwater**. Sannasiraj et al. (1998) conducted detailed experimental and theoretical investigations to study the behavior of pontoon-type floating breakwater. He measured the motion responses and mooring forces for three different mooring configurations as shown in Figure 2.2 below. It was found that the experimental measurements are consistent with the theoretical measurements, except for the roll resonance frequency. The results also indicated that the mooring line configurations will significantly affect the mooring forces but not the wave transmission coefficient.

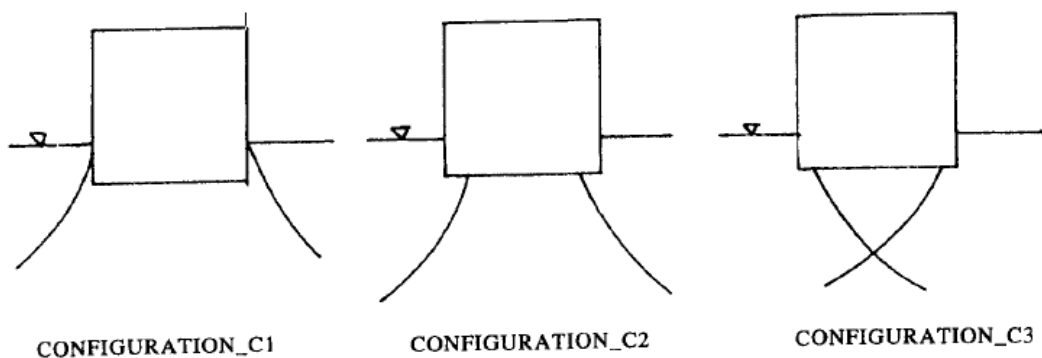


Figure 2.1: Mooring line configurations for single pontoon floating breakwater (Sannasiraj et al., 1998)

To reduce the wave transmission coefficient, many other floating breakwaters based on pontoon are being designed. Williams and Abul-Azm (1997) did an investigation on the hydrodynamic properties of **double pontoon floating breakwater**. The only difference between the single pontoon and dual pontoon breakwaters is that the latter one can reduce more waves due to turbulences between the two floating pontoons. They stated that the wave reflection properties of this type of floating breakwater depend on the draft and spacing of the pontoons, and also the mooring line stiffness. A study done by Ji et al. (2015) showed that the double pontoon floating breakwater can dissipate wave energy with short waves efficiently, but not the long waves.

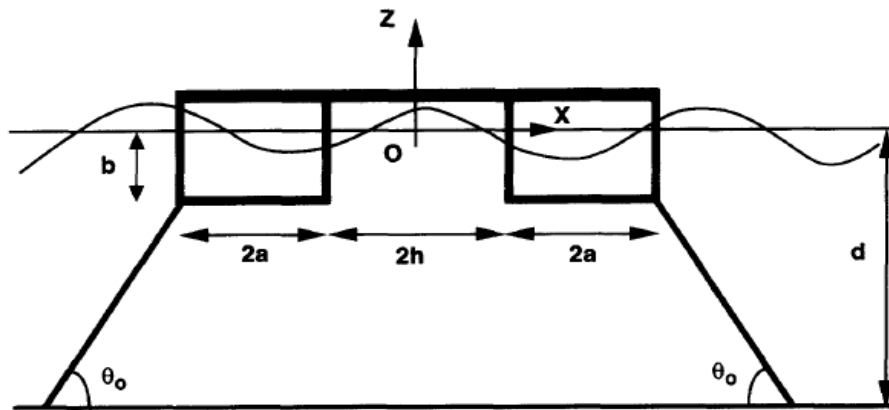


Figure 2.2: Dual pontoon breakwater sketch (Williams and Abul-Azm, 1997)

He et al. (2012) carried out experiment to investigate the hydrodynamic performances of **rectangular floating breakwater with and without pneumatic chambers**. The configuration consists of a rectangular box-type floating breakwater, with pneumatic chambers or oscillating water column (OWC) units attached to the front and back side of the original box-type breakwater. The pneumatic chamber used in the study was a hollow chamber with a large submerged bottom opening below the water surface. This concept originates from the oscillating water column (OWC) device that is commonly used in wave energy utilization (Falcao, 2010). The experimental results proved that the pneumatic chambers managed to reduce the wave transmission and significantly enhanced the wave energy dissipation. This is due to the presence of water in the chambers that helped to reduce the surge response plus the chamber walls that increased the moment of inertia of the breakwater and hence, mitigated the pitch response as well.

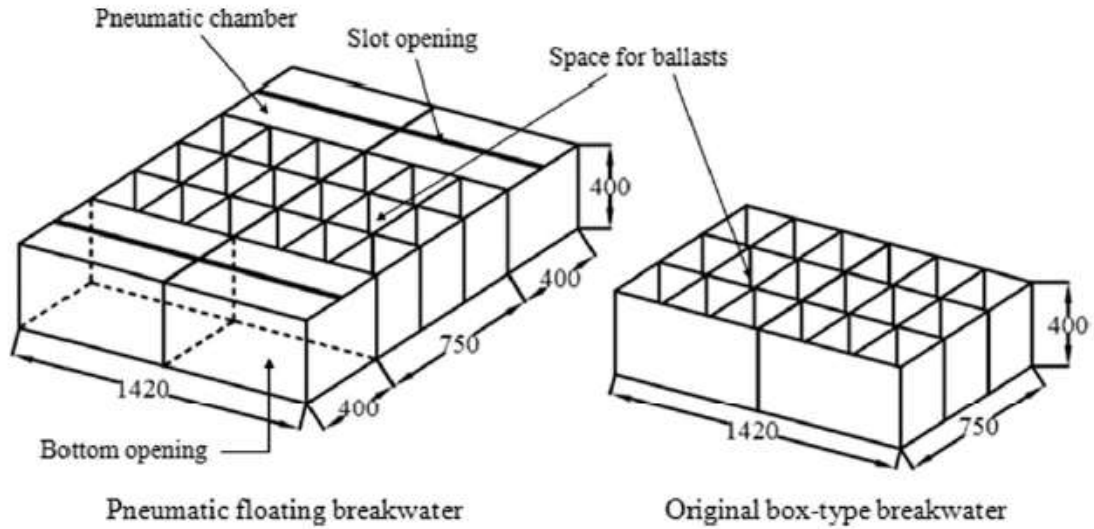


Figure 2.3: Pneumatic floating breakwater and original rectangular breakwater (He et al., 2012)

Since researchers found out that most of the wave energy is under the waterline, they started to develop floating breakwaters that can disturb the water particle orbit. Gesraha (2006) did an analysis on the **II Shaped Floating Breakwater**. It is a rectangular floating breakwater with two thin side-boards protruding vertically downward, like the shape of Greek letter II. By comparing to a normal rectangular breakwater, he concluded that such configuration will result in higher added mass and heave damping coefficient, but it actually lowered other damping coefficients, which resulted in smaller responses and transmission coefficient.

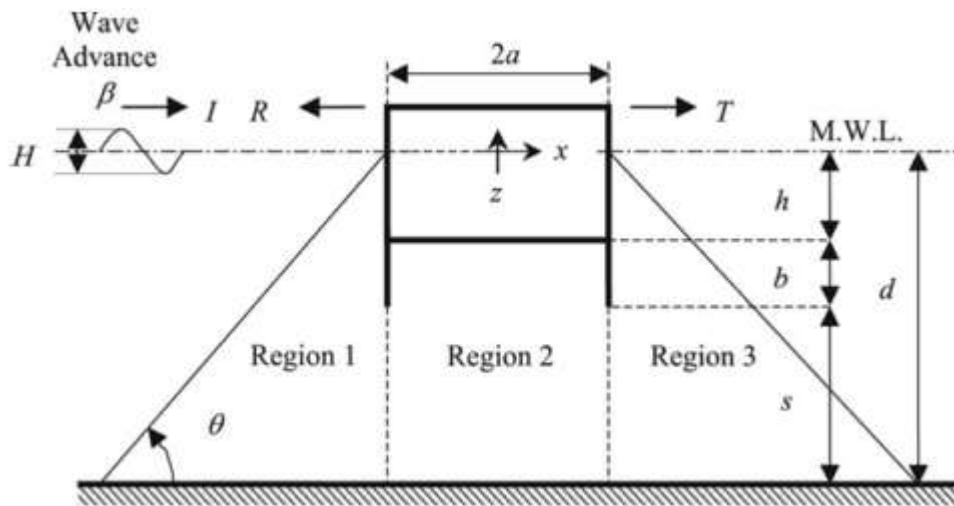


Figure 2.4: Schematic diagram of  $\pi$  shaped floating breakwater (Gesraha, 2006)

Studies by various researchers in the past have revealed that in order to achieve a transmission coefficient of less than 0.5, the  $B/L$  ratio ( $B$  is the width of the breakwater and  $L$  is the wave length) should always be greater than 0.3. However, Mani (1991) designed a **Y-frame floating breakwater** which has a  $B/L$  ratio of only 0.15 and yet the transmission coefficient is found to be less than 0.5. He added a row of cylinders with suitable length under a trapezoidal pontoon. The row of cylinders attached at the bottom of the structure has helped to increase the reflection characteristics of the structure as well as the level of turbulence. It was concluded that the width of the floating breakwater can even be reduced without affecting the transmission coefficient.

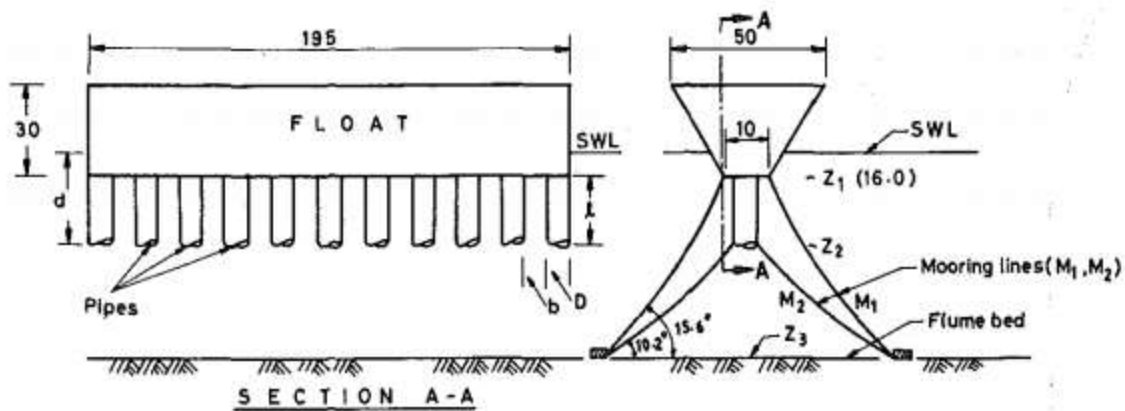


Figure 2.5: Details of Y-framed floating breakwater (Mani, 1991)

Since flexible structures are more convenient and cheaper compared to fixed-structures, studies have been done by researchers to develop floating breakwaters with flexible structures (McCartney, 1985). Dong et al. (2008) conducted a two-dimensional physical model test to measure the wave transmission coefficient of the **board-net floating breakwater**. The results showed that this type of floating breakwater can effectively reduce current velocity, which is beneficial for the fish in the cage. Therefore, this simple and yet inexpensive board-net floating breakwater is suitable to be used in aquaculture engineering. He also found out that the width of the board affects the wave transmission coefficients and the performance of the breakwater. The width should be chosen carefully depending on the conditions of the site where it will be used.

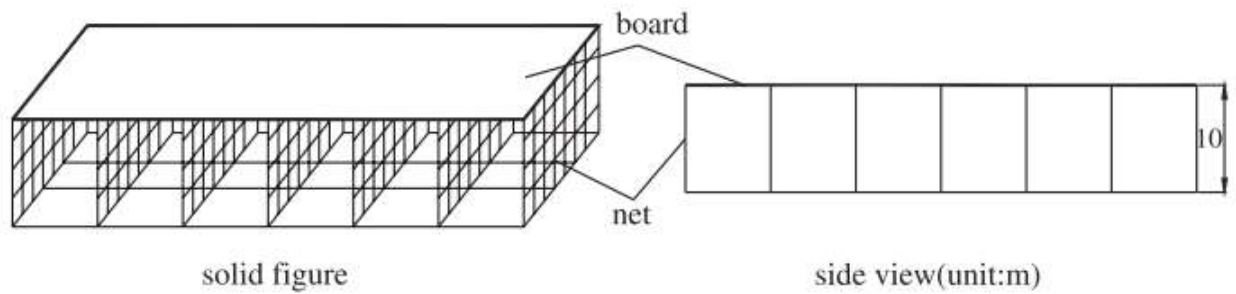


Figure 2.6: Board-net floating breakwater (Dong et al., 2008)

Teh and Mohammed (2012) studied the hydraulic performance of a newly developed floating breakwater, the **H-type floating breakwater (H-Float)** in regular waves. The wave transmission, reflection and energy dissipation characteristics of the breakwater model under various wave conditions were determined. The breakwater model was made of autoclaved lightweight concrete (ALC) with fiberglass coating. The purpose of the two “arms” at the top of the breakwater were to facilitate wave breaking at the structure; whereas the two “legs” at the bottom were designed in such a way that they will enhance the weight of the breakwater against wave actions. The experimental results showed that the wave transmission coefficient,  $C_t$  decreased with increasing B/L ratio (B is the width of the breakwater and L is the wave length). The H shaped floating breakwater is capable of attenuating up to 90% of waves when the B/L ratio is approaching 0.6.

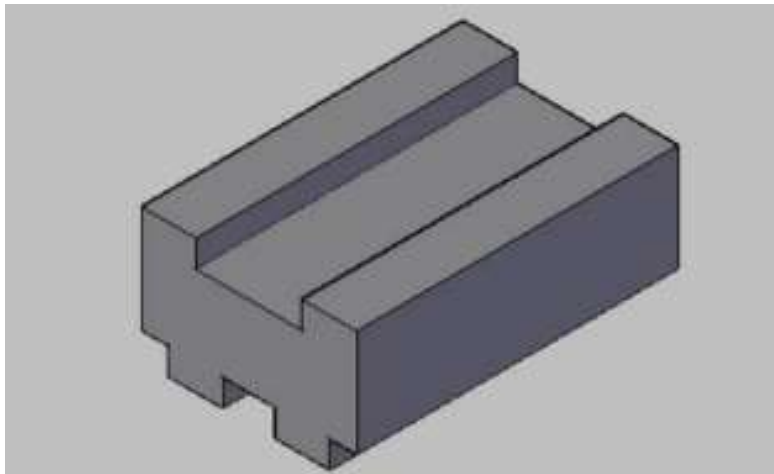


Figure 2.7: H shaped floating breakwater (Teh and Mohammed, 2012)

Ji et al. (2015) proposed a new type of floating breakwater which was named **Cylindrical Floating Breakwater (CFB)**. It consists of two parts: a main body of rigid cylinders and a flexible mesh cage containing a number of suspending balls that are intended to absorb the wave energy into their mechanical energy. Through comparison to double pontoons floating breakwater model, box floating breakwater model and the new CFB model only with the mesh cage, it was found that the new CFB with both mesh cage and the balls will increase the tension on the mooring lines and the sway motion. Nevertheless, it has the best performance in wave attenuation and can improve the efficiency of the floating breakwater, especially in long and high waves. It was proven that wave transmission can be significantly reduced with the presence of the mesh cage and the balls.

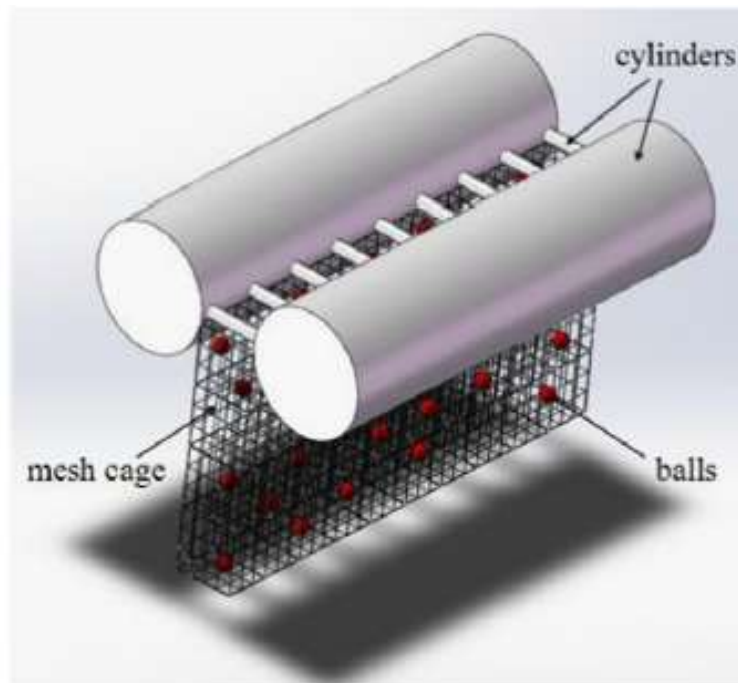


Figure 2.8: 3D sketch of Cylindrical Floating Breakwater (Ji et al., 2015)

All the existing floating breakwaters discussed earlier all have one major disadvantage in common, which is the inability to be rapidly installed at site. Some of these existing structures are big and bulky whereas some are made up of multi parts, which caused the installation works to be time consuming. Due to operations like the Logistics Over the Shore (LOTS) operation and the “Change of Pilot” operation in offshore, the demand of floating breakwater that can be rapidly installed has increased. The U.S. Army Engineer Research and Development Center (ERDC) has developed **Rapidly Installed Breakwater (RIB) System** to serve military purposes particular during the LOTS operation. During this operation, supplies and cargo from the deep draft Sealift ships are being offloaded onto smaller crafts termed lighter to be transported to smaller harbors or ports. For this operation to be conducted safely, the water height must be in sea states where the wave height is less than 1 meter (Briggs, 2001). Therefore, RIBS was designed to provide a calm basin at the leeward side of the structure. A report published by Dabling (2003) indicates that XM 2000 RIB can attenuate waves by about 70 percent. Nevertheless, transportability, the joint between the two arms of the V-shape and the hull strength are a few design characteristics that need to be further examined and improved.



Figure 2.9: Rapidly Installed Breakwater (RIB) System developed by U.S. Army (Briggs, 2001)

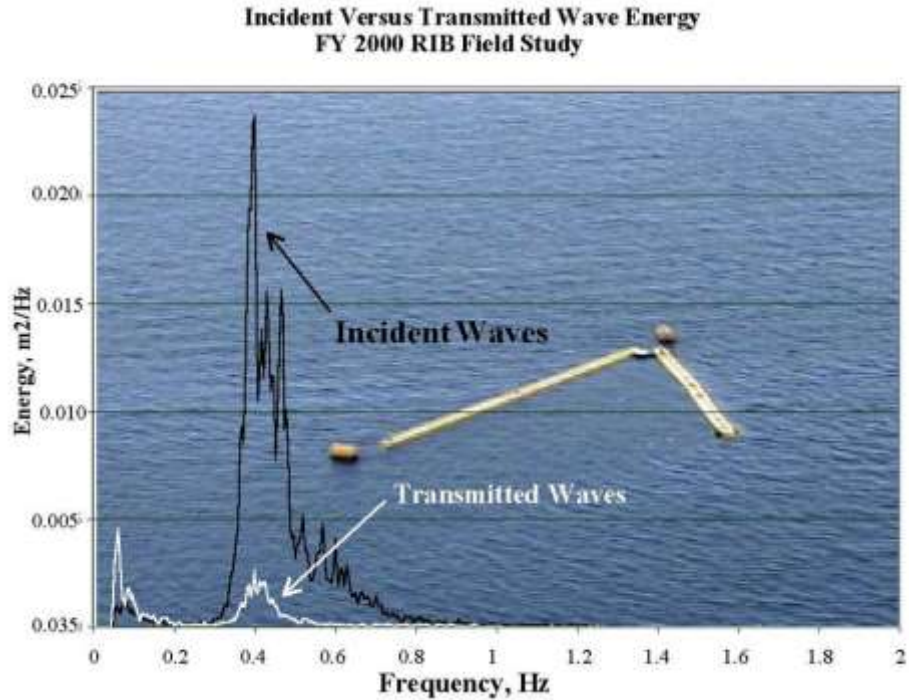


Figure 2.10: Change between the incident wave energy and the transmitted wave energy of XM 2000 RIB (Gobling, 2003)

Some of the other floating breakwaters available in the market nowadays that can be rapidly installed are **WaveEater**, **WhisprWave®** and **Wavebrake**. WaveEater is being developed as a rotationally moulded drum with baffles. It is an economical and durable wave attenuation system. However, its dissipation rates vary according to how the wave attenuation system is designed.



Figure 2.11: WaveEater

According to [www.whisprwave.com](http://www.whisprwave.com), the Whisprwave wave attenuator is able to dissipate 4-foot waves to 6 inches and achieve a 90% efficiency. The proprietary flexible backbone allows the system to work effectively and withstand substantial environmental forces. One of the highly attractive features of Whisprwave is that it can be submerged four to six feet below the freeze-line during winter, contributing to a minimal maintenance and reinstallation costs.



Figure 2.12: WhisprWave®

The Wavebrake has multiple voids that will dissipate the wave energy by hydraulic resistance and friction. This modular type floating breakwater can be configured into different kind of configurations. A typical system (2x3x2) can attenuate a 2' to 4' wave. The website <http://www.wavebrake.com/> stated that the Wavebrake is designed to achieve an 80% reduction in wave height.



Figure 2.13: Wavebrake

## 2.4 SCALING LAWS FOR SCALE EFFECTS

A physical hydraulic model is a scaled representation of a prototype. If the model displays similarity of dimension (geometric similarity), similarity of motion (kinematic similarity) or similarity of motion (dynamic similarity), the flow condition can be said to be similar. The forces that are acting on the waves are inertial, gravitational, viscous, elastic, pressure, and surface tension forces. According to Dalrymple (1985), the forces that are most relevant to most hydrodynamic problems are gravitational, friction and surface tension. Therefore, the dimensionless products are the combination of the Froude, Reynolds and Weber numbers.

### 2.4.1 Froude Number

Froude number is the ratio between inertial and gravitational forces. It measures the relative importance of inertial forces acting on a fluid particle to the weight of the particle (Hughes, 1993). It is normally used for scaling free surface flows or open channel hydraulics where the gravitational effects are always important and the friction effects are negligible. Gravity and most fluid characteristics are almost equivalent in both model and prototype, therefore if the contrary is not specifically mentioned; it can be assumed that they are being maintained.

$$Fr = \frac{V}{\sqrt{gL}} \quad (2.9)$$

where,

$Fr$  is Froude number,

$V$  is velocity,

$g$  is gravitational acceleration, and

$L$  is length.

$$Fr = 1, \quad \text{critical flow,}$$

$$Fr > 1, \quad \text{supercritical flow (fast rapid flow),}$$

$$Fr < 1, \quad \text{subcritical flow (slow / tranquil flow)}$$

During critical flow where the celerity is same as the flow velocity, any disturbance to the surface will remain stationary. However, in subcritical flow, backwater effects will occur. This is because the flow is controlled from a downstream point and the disturbance will be transmitted upstream. As for supercritical flow, the flow is being controlled upstream and disturbances will be transmitted downstream.

## 2.4.2 Reynolds Number

Reynolds number is the ratio between inertial forces and viscosity of a particle. It is usually being used in air models, intake structures, seepage flows or fully-enclosed flow where head losses are present. The typical Reynolds Number ( $Re$ ) is defined as:

$$Re = \frac{\rho VL}{\nu} \quad (2.10)$$

where,

$Re$  is Reynolds number,

$\rho$  is fluid density

$L$  is length,

$V$  is velocity,

$\nu$  is kinematic viscosity.

Reynolds number is used to determine the state of the flow in accordance to the following standards:

$Re < 2300$ : Laminar Flow

$2300 < Re < 4000$ : Transient Flow

$Re > 4000$ : Turbulent Flow

Laminar flow has a high viscosity due to the domination of viscous forces over the inertial forces. The behavior of the fluid depends mostly on its viscosity and the flow is steady or smooth. On the other hand, turbulent flow has low viscosity where the inertial forces dominate the viscous forces. The flow tends to be unsteady and churning.

### 2.4.3 Weber Number

Weber number is the ratio among inertia and surface tension forces. According to Martin and Pohl (200), surface tension is often neglected in most prototypes in hydraulic engineering; nevertheless, it is relevant in studies that are involving air entrainment (wave breaking), small waves (capillary waves) and shallow water depth.

$$W = \frac{\rho V^2 L}{\sigma} \quad (2.11)$$

where,

$W$  = Weber number

$L$  = length

$V$  = velocity

$\sigma$  = surface tension

$\rho$  = fluid density

## CHAPTER 3

### METHODOLOGY

#### 3.1 GENERAL

This chapter will provide the details of the physical model (modules) and the laboratory equipment that will be used to conduct this study. Besides that, the experimental set-up will also be included in this chapter. Last but not least, the flow chart, Gantt chart and key milestones of this study are shown at the end of this chapter.

#### 3.2 PHYSICAL MODEL

The physical model consisted of interlocking modules of two shapes. There were 8 rectangular-shaped modules and 2 triangular-shaped modules (right-angled). The dimensions of both the modules are shown in figures below (Figure 3.1 to figure 3.6).

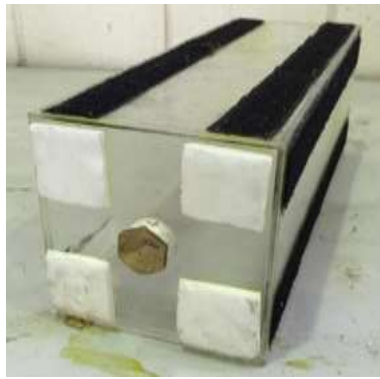


Figure 3.1: Rectangular-shaped module

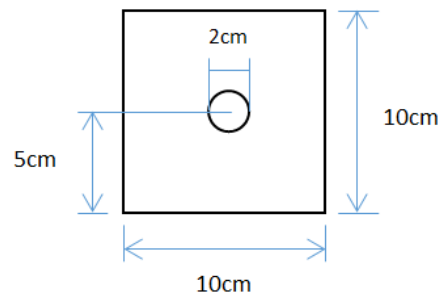


Figure 3.2: Front view of rectangular-shaped module

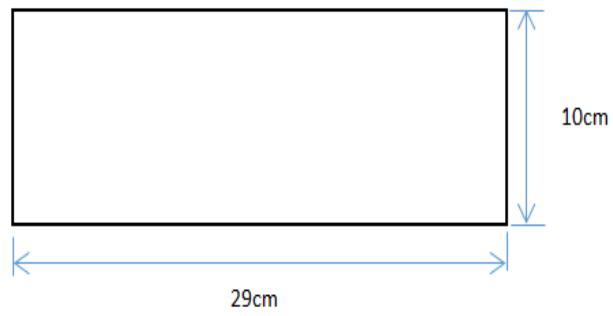


Figure 3.3: Right side view of rectangular-shaped module

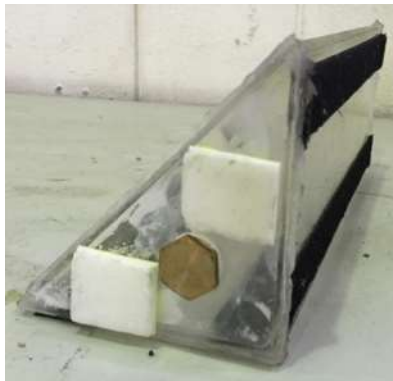


Figure 3.4: Triangular-shaped module

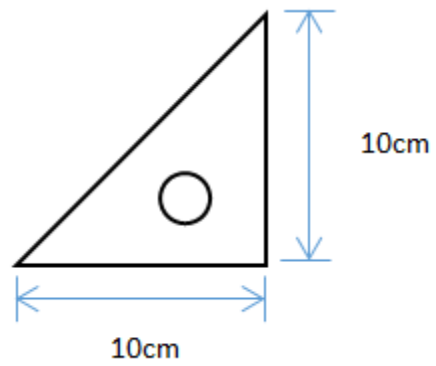


Figure 3.5: Front view of triangular-shaped module

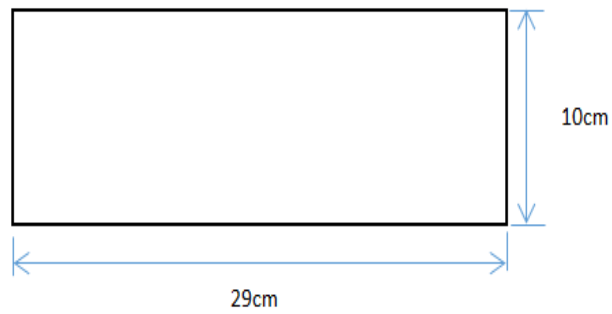


Figure 3.6: Right side view of triangular-shaped module



Figure 3.7: Brass stop pipe plug

These modules can be assembled and connected in many different ways to construct the breakwater structure. These modules can be filled with air, water or other fluids of higher density to control the buoyancy of the structure. With this, the draft of the floating breakwater can also be manipulated.

### 3.3 LABORATORY EQUIPMENT AND INSTRUMENTS

#### 3.3.1 Wave Flume

The experiments were being carried out in a wave flume in Universiti Teknologi PETRONAS (UTP). The flume had a dimension of 10m length, 31cm width and 48cm height. Its effective working depth (maximum water depth before water splashes out when wave generator is in use) was 30cm. It had a rigid bed and the sides were lined with glass panels for the entire length of the flume for observation of the experiment inside the flume. Regular waves were being generated by a wave paddle (wave generator).



Figure 3.8: Wave flume

#### 3.3.2 Wave Paddle

Wave paddle is a wave generator which was installed at one end of the wave flume that can generate both regular and irregular waves for laboratory testing purposes. It had the capability to generate waves up to 2 second wave period and maximum wave height of 0.3 meter. The manufacturer of this wave paddle is G.U.N.T. (Germany). During the experimental run, the waves that were reflected back were absorbed by this wave paddle through the use of force feedback system.



Figure 3.9: Wave paddle

### 3.3.3 Wave Absorber

A wave absorber is an inclined plane with sponge at the upper surface. It was used to absorb the remaining wave energy that reached the end of the wave flume. Reflection of waves at the end of the wave flume must be avoided. The occurrence of such reflection will alter the wave height and ultimately affecting the readings of the measured wave heights. The wave absorber being used for this study is shown in Figure 3.10 and Figure 3.11 below.



Figure 3.10: Wave absorber



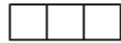
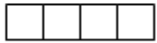
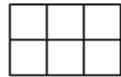
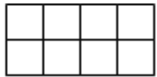
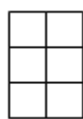
Figure 3.11: Wave absorber (side view)

### 3.4 EXPERIMENTAL SET-UP

The tests took place in the Hydraulic Laboratory which is situated in Block J of Universiti Teknologi PETRONAS (UTP). The modules were arranged and connected to form several physical models with different shapes or configurations. Two mooring lines were being placed at the wave-ward side of the test model and another two at the lee-ward side to connect the test model to the bottom hook. Book straps made of Velcro were being used as cables to hold the modules together and also act as the attachment points between the mooring lines and the floating structure. The goals of the experiments were to study the effect of: (i) breakwater width and draft and (ii) different irregular configurations. All the shapes and configurations of physical models are shown in Table 3.1 and Table 3.2 below.

#### Experiment 1: Effect of breakwater width and draft

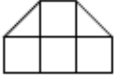
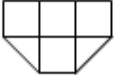
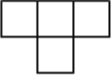
Table 3.1: Arrangements of physical models to evaluate the effects of breakwater width and draft on wave transmission characteristics of the rapidly installed modular floating breakwaters

	1 column	2 columns	3 columns	4 columns
Single layer	 Model 1x1	 Model 1x2	 Model 1x3	 Model 1x4
Double layer	 Model 2x1	 Model 2x2	 Model 2x3	 Model 2x4
Triple layer	 Model 3x1	 Model 3x2		

This experiment was to evaluate the effects of breakwater width and draft on wave transmission characteristics of the rapidly installed modular floating breakwaters in regular waves. In this experiment, only the rectangular-shaped modules were used to form floating breakwaters with different draft and width.

## Experiment 2: Effect of irregular breakwater configurations

Table 3.2: Arrangements of physical models to compare wave attenuation performance of the rapidly installed modular floating breakwaters of different irregular configurations

	Configuration 1	Configuration 2	Configuration 3	Configuration 4	Configuration 5
Matrix 2x2	 Model 1A	 Model 1B	 Model 1C	 Model 1D	 Model 1E
Matrix 2x3	 Model 2A	 Model 2B	 Model 2C	 Model 2D	

This experiment was to compare wave attenuation performance of the rapidly installed modular floating breakwaters of different irregular configurations in regular waves. In this experiment, both the rectangular-shaped and triangular-shaped modules were used to form breakwaters which are in the matrix form of 2 x 2 and 2 x 3.

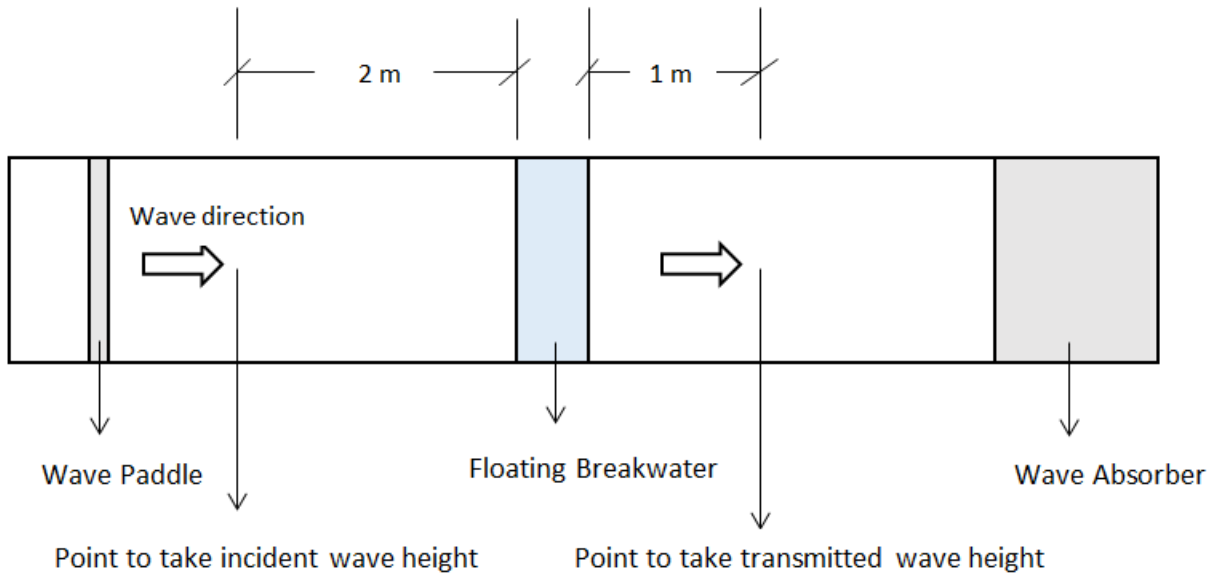


Figure 3.12: Experiment set-up (plan view)

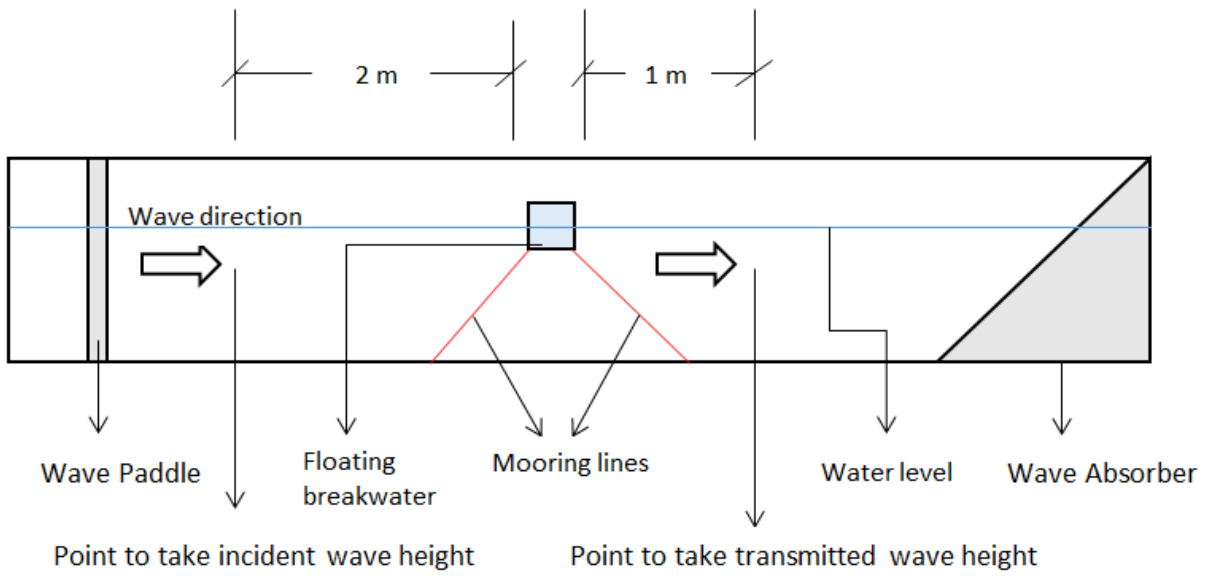


Figure 3.13: Experiment set-up (side view)

The incident wave height and transmitter wave height were being taken manually by measuring the vertical distance between the crest and the trough of the third wave generated by the wave paddle using a ruler. The crest and trough of the waves were observed through the glass panels at the side of the wave flume. For each wave period and stroke adjustment, the incident and transmitted wave height were being measured for three times and the average of the three values was used as the final result. This was done to ensure that the results were highly reliable and accurate.

In every research study, there are some constant and manipulated parameters. It is very important for these parameters to be known even before the study begins. The constant and manipulated parameters for this study have been tabulated in the table below.

Table 3.3: Parameters used in the experiment

Constant Parameters	Manipulated Parameters
Water depth, $d$ (30cm)	Wave period, $T$ or wavelength, $L$
Mooring configurations (taut-leg mooring)	Incident wave height, $H_i$
Wave type (regular)	Stroke adjustments
	Breakwater geometry: Width, $B$ and draft, $D$
	Breakwater configurations: 2 x 3 and 3 x 3 matrix

The physical models were being tested in the wave flume with wave period ranging from 0.8s to 1.6s with 0.4 second interval and stroke adjustment of 40mm, 120mm and 200mm. The total number of test runs for this study was 171 (19 models x 3 wave period x 3 stroke adjustments) and all these test runs were being subjected to unidirectional regular waves only. Table 3.4 shows the wave condition under the water depth of 30cm.

Table 3.4: Wave condition at water depth of 30cm

Water depth, $d$ (cm)	Period, $T$ (s)	Wavelength, $L$ (m)	Stroke Adjustment (mm)
30	0.8	0.96	40, 120, 200 (1 cm < $H_i$ < 6.5cm)
	1.2	1.77	
	1.6	2.53	

The parameters listed in the table are water depth ( $d$ ), wave period ( $T$ ), wavelength ( $L$ ) and wave height ( $H_i$ ). The value of wavelength ( $L$ ) can be obtained from Table C1: Shore Protection Manual, Wiegel (1948) after the calculation of  $d/L_o$ . The relationship of these parameters is shown below:

$$L_o = gT^2/2\pi$$

Equation 1: Relationship between wave parameters

At the end of the experimental tests, results were compiled and analysed based on the wave transmission coefficient,  $C_t$  value.  $C_t$  represents the ratio of transmitted wave height to the incident wave height. It can be used to quantify the degree of wave attenuation of the floating breakwater. A low  $C_t$  value simply means that smaller waves are being transmitter beyond the structure. Therefore, the lower the  $C_t$  value, the better the wave attenuation performance of the floating breakwater.

### 3.5 FLOW CHART

A series of activities were carried out to ensure that the research study is correctly and successfully done. These procedures were done in stages so that the flow of the study will not be obstructed. The procedures are as follows:

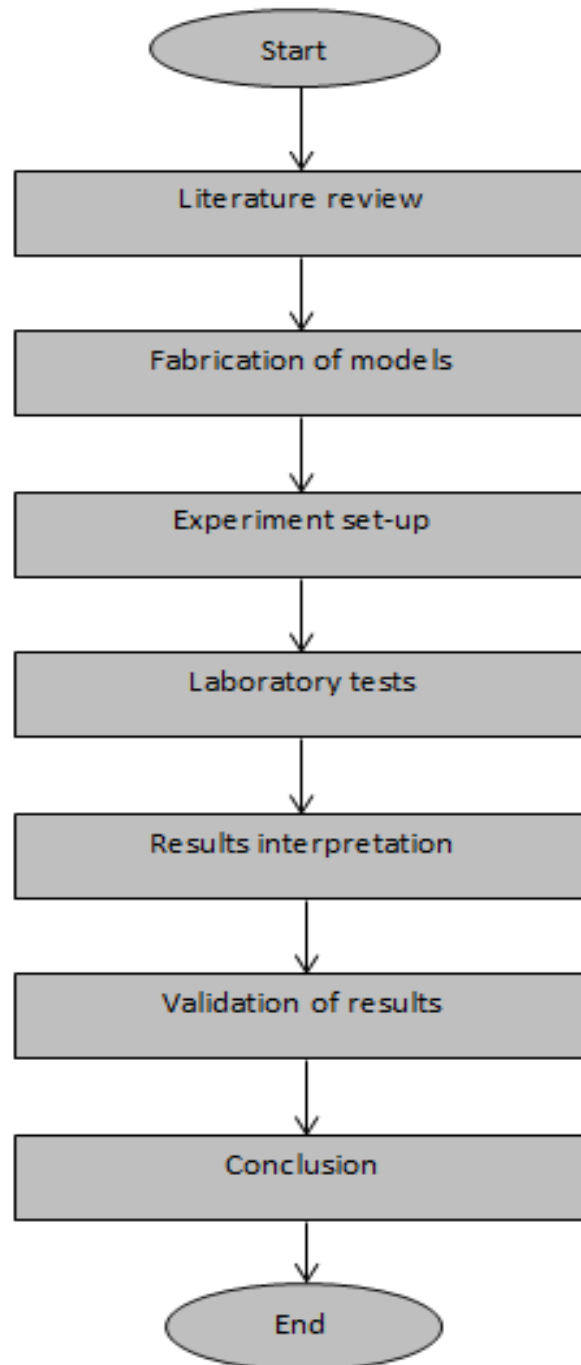


Figure 3.14: Procedures conducted

### 3.6 GANTT CHART

Table 3.5: Gantt Chart

Task/Activity	FYP 1 Week No.														FYP 2 Week No.													
	1	2	3	4	5	6	7	8	9	10	11	12	13	14	1	2	3	4	5	6	7	8	9	10	11	12	13	14
Selection of project title	█																											
Research work	█	█	█	█	█																							
Submission of extended proposal						█																						
Continuation of report							█	█																				
Proposal defense									█																			
Design and fabrication of floating breakwater										█	█	█	█															
Submission of draft interim report													█															
Submission of interim report														█														
Laboratory tests															█	█	█	█	█	█	█							
Submission of progress report																						█						
Continuation of report																							█	█	█			
Pre-SEDEX																									█			
Submission of draft final report																										█		
Submission of technical report (final report)																										█	█	
Viva																										█	█	
Submission of dissertation																											█	

### 3.7 KEY MILESTONE

- Final Year Project 1 (FYP 1)

Table 3.6: Key milestone for FYP 1

Milestone	Week
Selection of title	Week 1
Submission of extended proposal	Week 6
Proposal defense	Week 9
Submission of interim report	Week 14

- Final Year Project 2 (FYP 2)

Table 3.7: Key milestone for FYP 2

Milestone	Week
Submission of progress report	Week 8
Pre-SEDEX	Week 11
Submission of technical report	Week 13
VIVA	Week 13
Submission of Dissertation	Week 14

## CHAPTER 4

### RESULTS AND DISCUSSION

#### 4.1 GENERAL

This chapter will include the results of the experiments carried out to meet both objectives of this research study which are: (i) the effect of breakwater width and draft and (ii) the effect of different irregular configurations. The results will be presented by graphs of  $C_t$  values against wave steepness,  $H_i/L$  and also graphs of  $C_t$  values against relative width of breakwater,  $B/L$ . In addition to that, the details of the analysis of results will be thoroughly discussed in this chapter as well. These analyses are essential to provide a better understanding and interpretation of results at the end of this research study.

**Annotation:**

$H_t$	–	Transmitted wave height
$H_i$	–	Incident wave height
$L$	–	Wavelength
$B$	–	Breakwater width
$D$	–	Draft of breakwater
$d$	–	Water depth
$C_t$	–	Transmission coefficient ( $= H_t/H_i$ )
$H_i/L$	–	Wave steepness
$B/L$	–	Relative width of breakwater
$B/d$	–	Ratio of breakwater width to water depth
$D/d$	–	Relative draft of breakwater

## 4.2 EFFECT OF WAVE STEEPNESS

### 4.2.1 Experiment 1: Effect of breakwater width and draft

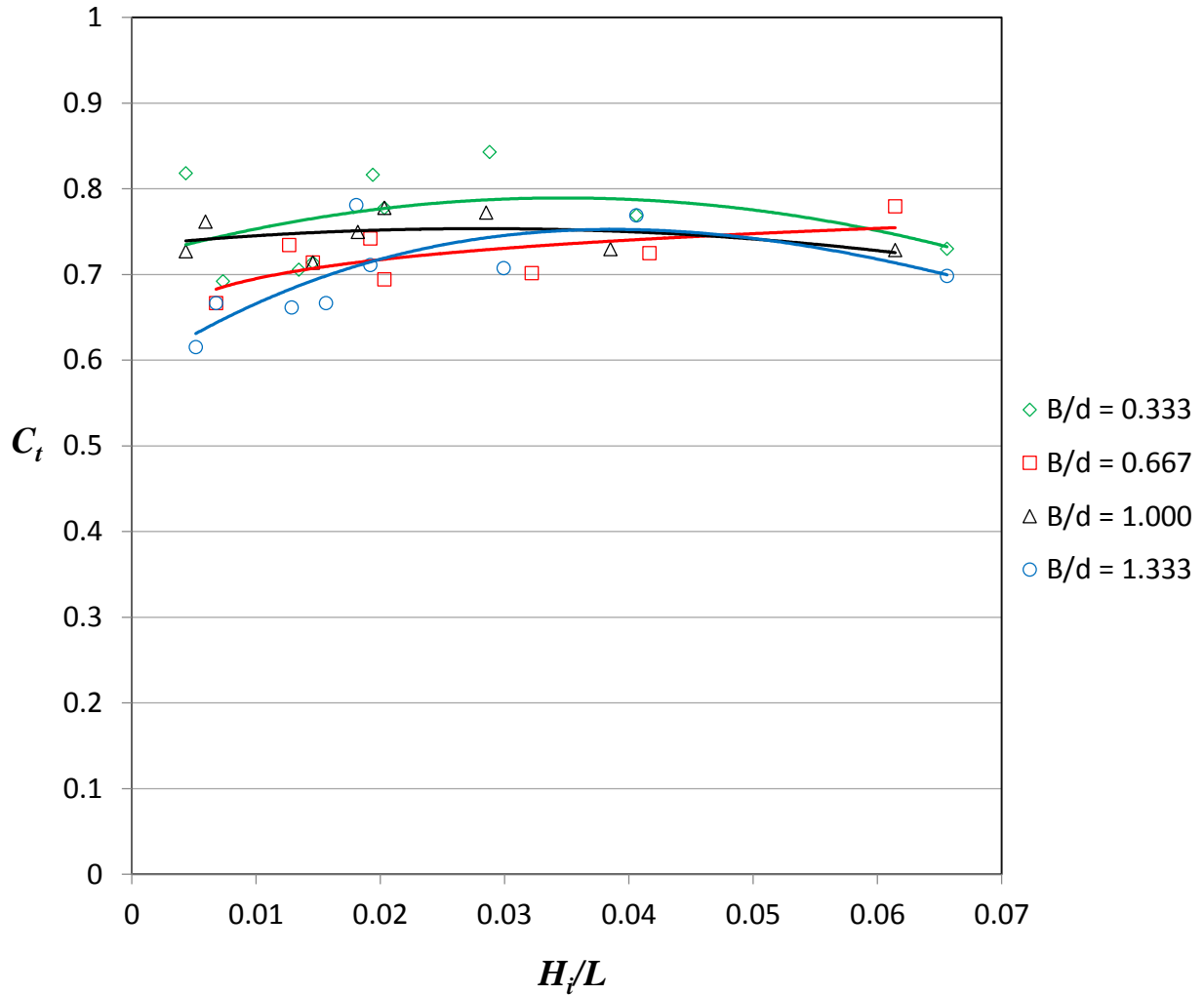
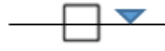
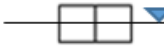
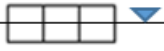
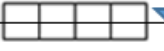


Figure 4.1: Effect of breakwater width on  $C_t$  of the single layer models ( $D/d = 0.167$ )

**Table 4.1: Test parameters for single layer models**

Layout Matrix	1 x 1	1 x 2	1 x 3	1 x 4
Configuration				
$D/d$	0.167	0.167	0.167	0.167
$B/d$	0.333	0.667	1.000	1.333

**Table 4.2: Statistics of  $C_t$  values for single layer models**

Model	$C_t$ Range	Mean $C_t$	Standard deviation
1 x 1	0.692 – 0.843	0.763	0.0551
1 x 2	0.667 – 0.780	0.720	0.0341
1 x 3	0.727 – 0.778	0.745	0.0236
1 x 4	0.615 – 0.781	0.698	0.0529

**Figure 4.1** represents variation in wave transmission coefficient with respect to wave steepness. Values of  $C_t$  vs  $H_i/L$  for single layer breakwaters of different widths are plotted. It can be seen from the plot that relationship between  $C_t$  and  $H_i/L$  is not significant for all models.  $C_t$  values do not show much variation with change in wave steepness. This can be explained by the fact that most of the incident waves used during the experimentation was smaller than height of the structure and were reflected back. Wave overtopping was only observed for waves with higher wave steepness ( $H_i/L > 0.06$ ) during the model testing. Although variation in  $C_t$  with respect to width of the structure is very small but still it is worth mentioning that models with smaller width gave higher  $C_t$  values whereas wider models gave comparatively lower wave transmission.  $C_t$  values varied between the ranges of 0.615 to 0.843 for all the models. Minimum  $C_t$  value of 0.615 was obtained by Model 1 x 4 which has the maximum width as compared to all the other models under consideration.

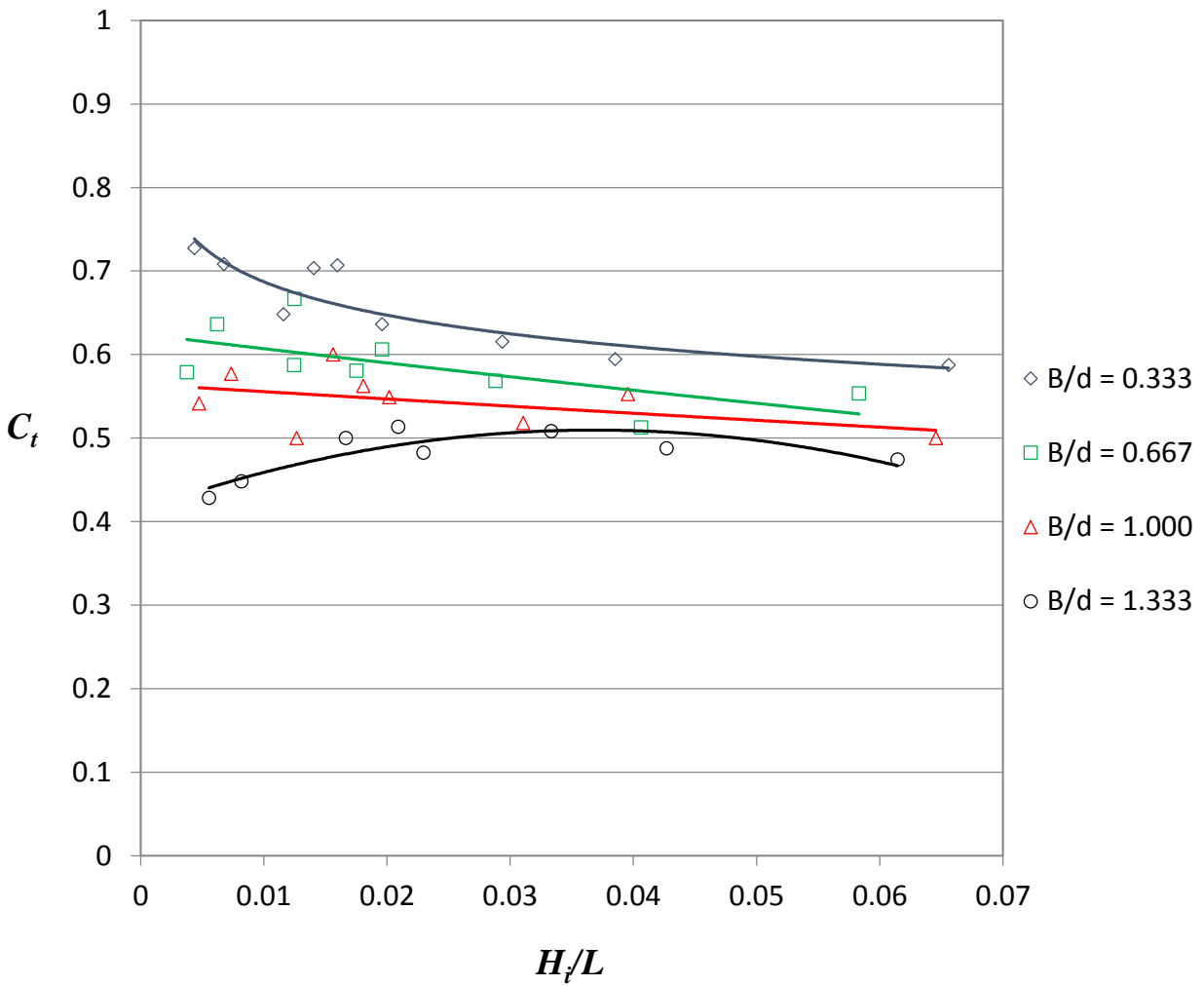


Figure 4.2: Effect of breakwater width on  $C_t$  of the double layer models ( $D/d = 0.333$ )

Table 4.3: Test parameters for double layer models

Layout Matrix	2 x 1	2 x 2	2 x 3	2 x 4
Configuration				
$D/d$	0.333	0.333	0.333	0.333
$B/d$	0.333	0.667	1.000	1.333

**Table 4.4: Statistics of  $C_t$  values for double layer models**

Model	$C_t$ Range	Mean $C_t$	Standard deviation
2 x 1	0.587 – 0.727	0.659	0.0538
2 x 2	0.513 – 0.667	0.588	0.0450
2 x 3	0.500 – 0.600	0.545	0.0339
2 x 4	0.429 – 0.514	0.481	0.0295

The variation in wave transmission coefficient with respect to wave steepness is being illustrated in **Figure 4.2**. Values of  $C_t$  vs  $H_i/L$  for double layer breakwaters of different widths are plotted. It can be seen from the plot that  $H_i/L$  has a mild effect on  $C_t$  values for all models. For models with  $B/d$  values of 0.333, 0.667 and 1.000,  $C_t$  values reduced slightly as the wave steepness increased from 0.01 to 0.07. However for model with the largest width ( $B/d = 1.333$ ),  $C_t$  values increased as wave steepness increased from 0.01 up to 0.03, but as the wave steepness keeps on increasing thereafter,  $C_t$  values actually showed a slight decrement. Besides that, effect of width of breakwater on  $C_t$  can be seen in this plot. Models with smaller width produced higher  $C_t$  values whereas wider models produced lower values of wave transmission coefficient. The  $C_t$  values varied between the ranges of 0.429 to 0.727 for all the models. Model which has the maximum width (Model 2 x 4) produced the minimum  $C_t$  value of 0.429. On the contrary, the model with the minimum width (Model 2 x 1) produced the maximum  $C_t$  value of 0.727.

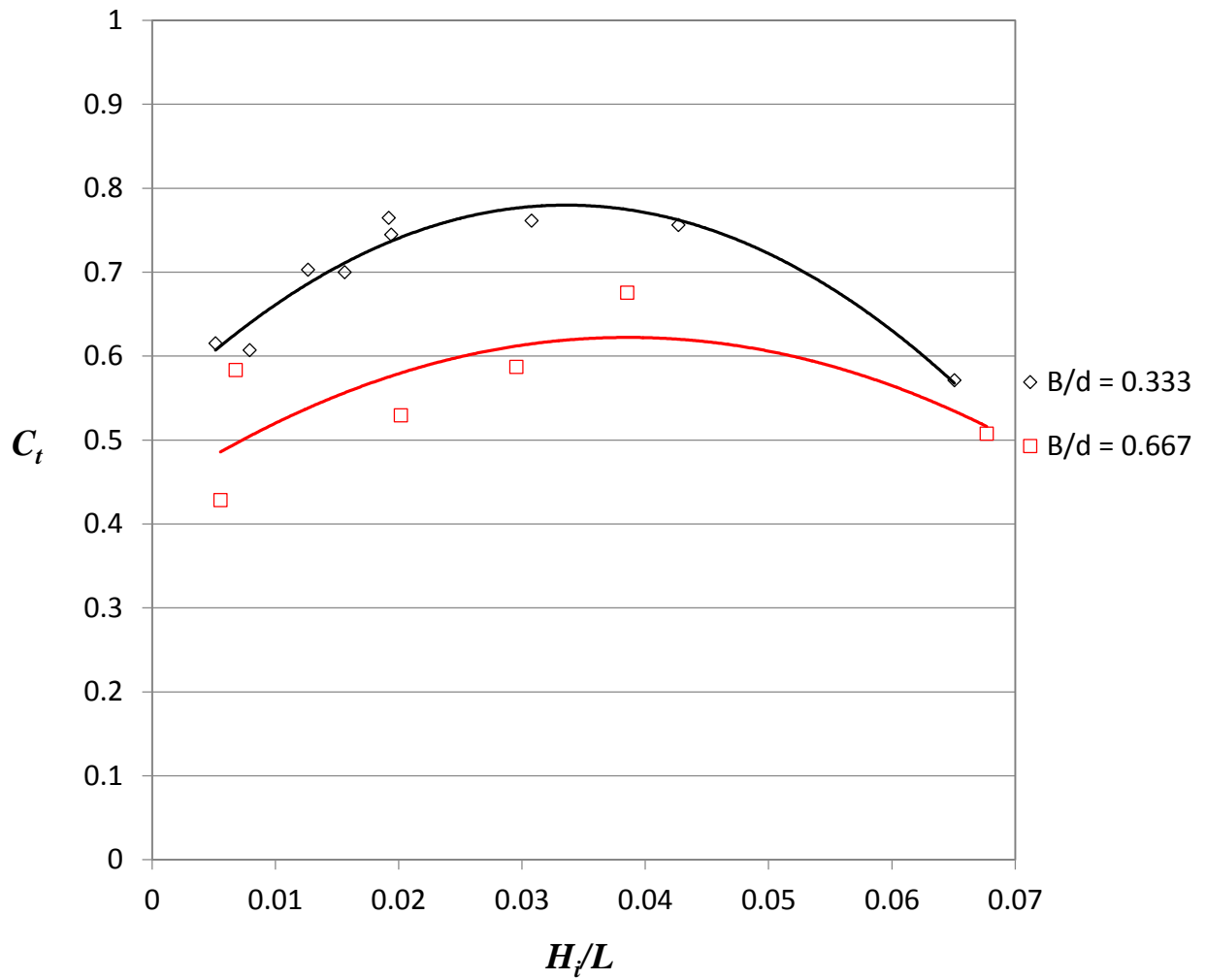


Figure 4.3: Effect of breakwater width on  $C_t$  of the triple layer models ( $D/d = 0.667$ )

Table 4.5: Test parameters for triple layer models

Layout Matrix	3 x 1	3 x 2
Configuration		
$D/d$	0.667	0.667
$B/d$	0.333	0.667

**Table 4.6: Statistics of  $C_t$  values for triple layer models**

Model	$C_t$ Range
3 x 1	0.571 – 0.765
3 x 2	0.429 – 0.676

**Figure 4.3** exhibits variation in wave transmission coefficient with respect to wave steepness. Values of  $C_t$  vs  $H/L$  for triple layer breakwaters of different widths are plotted. From the plot, it can be seen that  $H/L$  has a quite significant effect on  $C_t$  values for both models.  $C_t$  values of both models showed increment as the wave steepness increased from 0.01 to 0.03 and then started to decrease as the wave steepness keeps on increasing. This can be explained by the fact that when the wave steepness is small, most of the incident waves were being reflected back, therefore the low  $C_t$  values. As the steepness and size of wave increases, more waves were able to travel pass the structure, hence an increase in  $C_t$  values. However, as the wave steepness keeps on increasing until a certain extent, the waves tend to break even before they interact with the structure, causing the decrement of  $C_t$  values. Besides that, effect of width of breakwater on  $C_t$  can be clearly seen in this plot. Model 3 x 1 with a smaller width had higher  $C_t$  values whereas model 3 x 2 with a greater width had lower  $C_t$  values. The  $C_t$  values varied between the ranges of 0.429 to 0.765 for both the models.

#### 4.2.1.1 Summary

From the 3 graphs, it can be seen that with increase in wave steepness,  $C_t$  values remain almost constant for most of the structures. The models with  $D/d$  value of 0.167 had very high  $C_t$  values ranging from 0.65 to 0.85. The models with  $D/d$  value of 0.333 had relatively smaller  $C_t$  values ranging from 0.45 to 0.65. The models with  $D/d$  value of 0.667 had a very different behavior as compared models with other  $D/d$  values. With deeper draft, it was expected to have  $C_t$  values lower than the  $C_t$  values given by all the other models with shallower draft. The inconsistent behavior of these models can be due to large movements induced in the structure during the wave-structure interaction. Under waves of  $H/L$  from 0.02 to 0.05, the structure experienced very large movements. In turn, the models behaved as a wave generator and increased the transmitted waves. This can be concluded that although deeper draft enhanced wave attenuation ability of the structure, however the motion responses and mooring line configuration also play an important role.

### 4.2.2 Experiment 2: Effect of irregular breakwater configuration

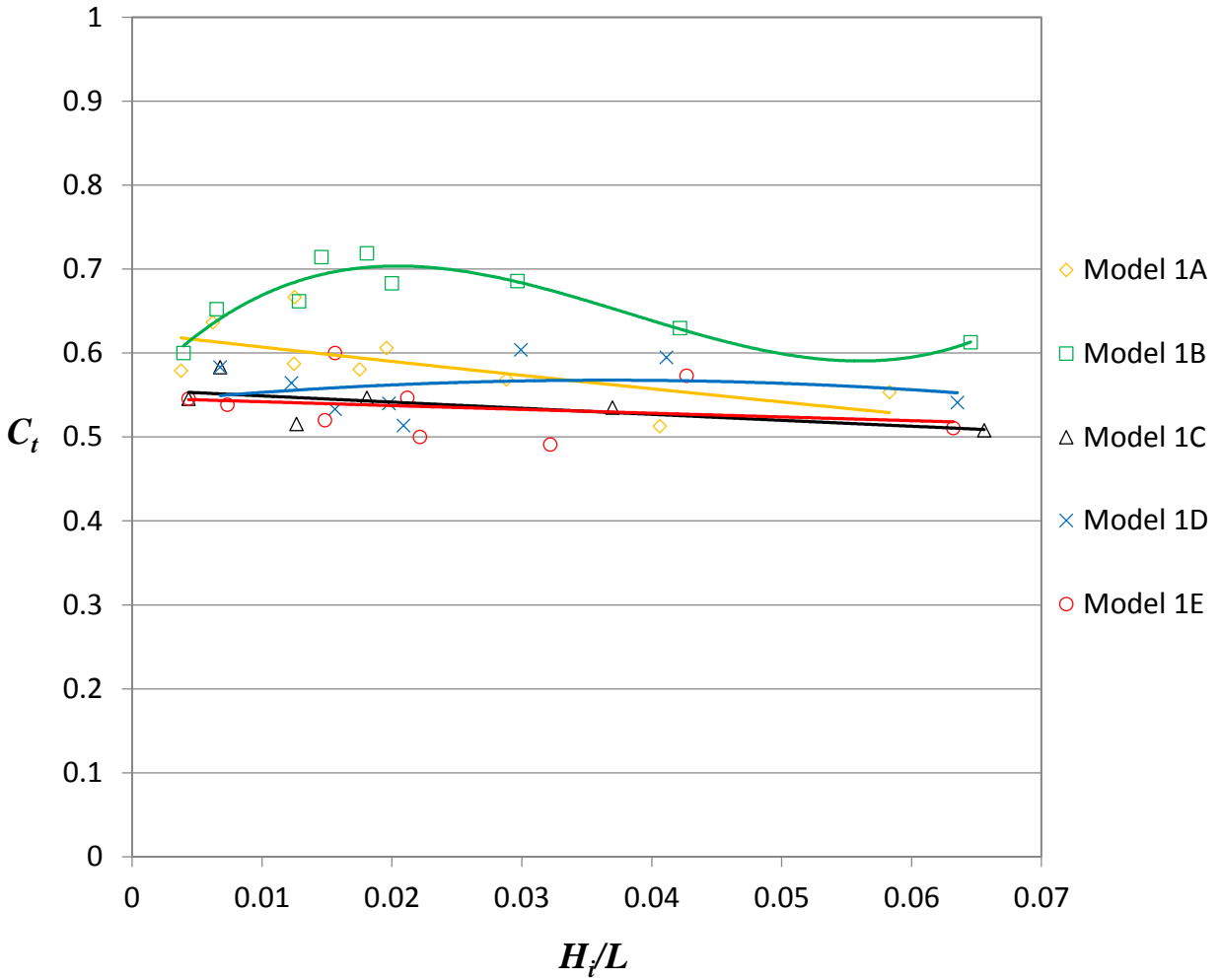
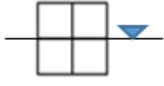
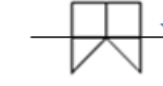


Figure 4.4: Effect of breakwater configuration on  $C_t$  of the 2 x 2 matrix models ( $D/d = 0.333$ )

**Table 4.7: Test parameters for 2 x 2 matrix models**

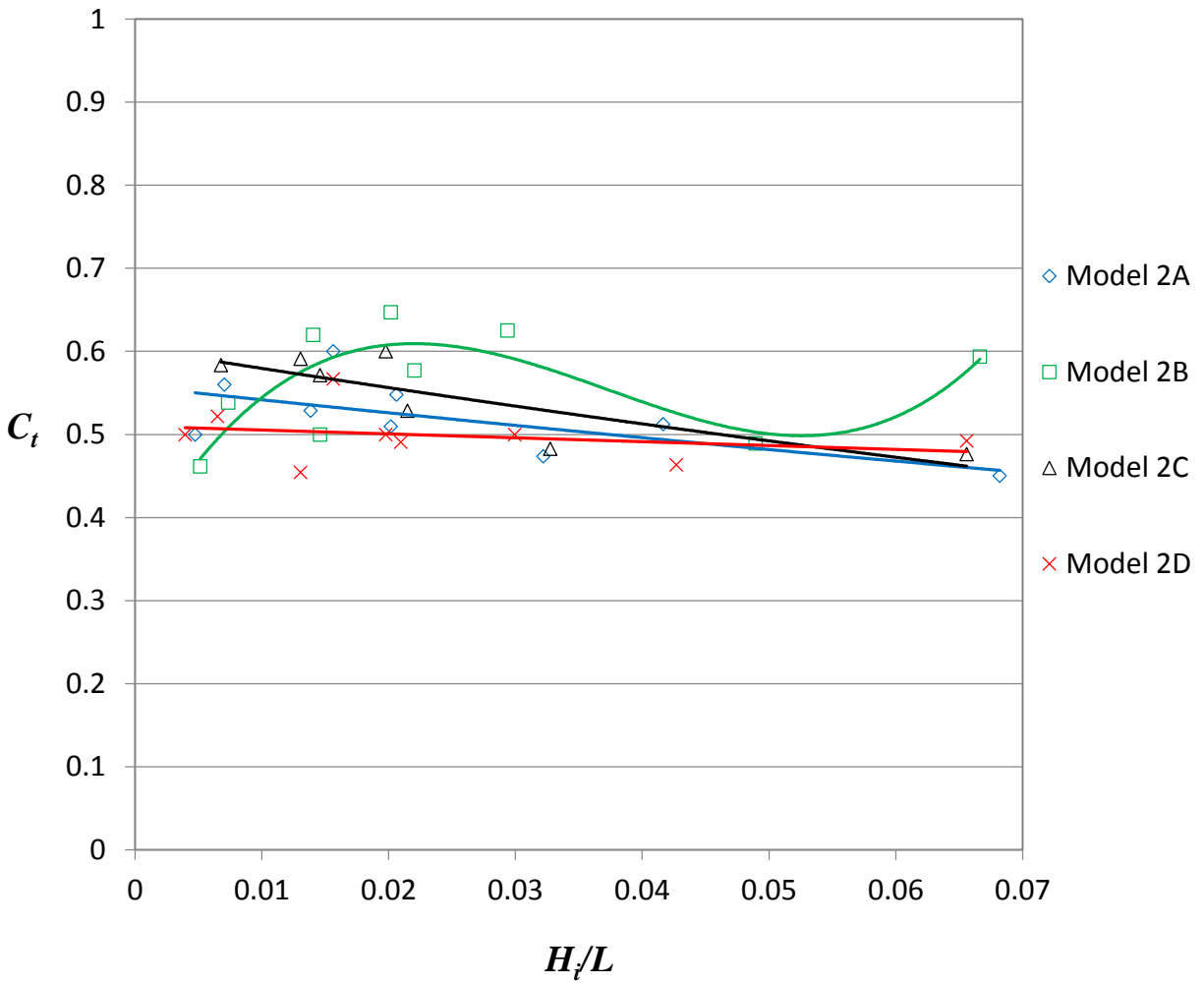
Matrix	1A	1B	1C	1D	1E
Configuration					
$D/d$	0.333	0.333	0.333	0.333	0.333
$B/d$	0.667	0.667	0.667	0.667	0.667

**Table 4.8: Statistics of  $C_t$  values for 2 x 2 matrix models**

Model	$C_t$ Range	Mean $C_t$	Standard deviation
1A	0.513 – 0.667	0.588	0.0450
1B	0.600 – 0.719	0.662	0.0424
1C	0.508 – 0.583	0.539	0.0268
1D	0.514 – 0.604	0.559	0.0324
1E	0.491 - 0.600	0.536	0.0352

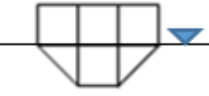
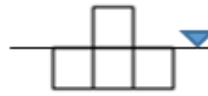
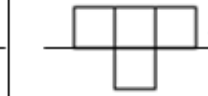
**Figure 4.4** indicates variation in wave transmission coefficient with respect to wave steepness. Values of  $C_t$  vs  $H_i/L$  for breakwaters with irregular configurations of 2 x 2 matrix are plotted. All the models are of the same width and draft. From the plot, it can be seen that  $H_i/L$  has very mild effect on  $C_t$  values for all the models except for model 1B. Model 1B with a hull shape base produced a completely different trend line compared to the others, which is sinusoidal shaped and the  $C_t$  values are relatively high as compared to all the other models under consideration, throughout various  $H_i/L$  values. This undesirable performance might be due to the low stability of the model which caused the rolling effect. Due to this effect, the structure actually acted like a paddle and generated extra waves at the leeside of the structure, hence causing the  $C_t$  values to be high.  $C_t$  values of the other four models (Models 1A, 1C, 1D and 1E) remain almost constant throughout various wave steepness values. The  $C_t$  values varied between the ranges of 0.491 to 0.667. Judging by the lower  $C_t$  values, it can be said the models 1C and 1E attenuated more waves than the others. This can be explained by the fact that the shape of the model 1C can dissipate more wave energy by allowing wave overtopping whereas the area between the two upper triangular arms of model 1E had the tendency to accumulate water when

the waves overtopped the structure, hence reducing the transmitted wave height and lowering the  $C_t$  values.



**Figure 4.5: Effect of breakwater configuration on  $C_t$  of the 2 x 3 matrix models ( $D/d = 0.333$ )**

**Table 4.9: Test parameters for 2 x 3 matrix models**

Matrix	2A	2B	2C	2D
Configuration				
$D/d$	0.333	0.333	0.333	0.333
$B/d$	1.000	1.000	1.000	1.000

**Table 4.10: Statistics of  $C_t$  values for 2 x 3 matrix models**

Model	$C_t$ Range	Mean $C_t$	Standard deviation
2A	0.450 – 0.600	0.520	0.0453
2B	0.462 – 0.647	0.561	0.0666
2C	0.476 – 0.600	0.548	0.0519
2D	0.455 – 0.567	0.499	0.0325

The variation in wave transmission coefficient with respect to wave steepness is shown in **Figure 4.5**. Values of  $C_t$  vs  $H_i/L$  for breakwaters with irregular configurations of 2 x 3 matrix are plotted. The width and draft of all the models are being kept constant. From the plot, it can be seen that  $H_i/L$  has a quite significant effect on  $C_t$  values for all the models. Model 2B with a hull shape base produced a completely different trend line compared to the others, which is sinusoidal shaped and the  $C_t$  values are relatively higher as compared to all the other models under consideration, throughout various  $H_i/L$  values. This can be related to the model 1B in figure 4, which has a similar sinusoidal trend line. This undesirable performance might be due to the same reason, which was the low stability of the model. During the wave-structure interaction, the structure actually experienced rolling effect and acted like a paddle which generated extra waves at the leeside of the structure, causing a high transmitted wave height. For the other 3 models (models 2A, 2C and 2D), the  $C_t$  values showed decrement of different degrees as wave steepness increased. Model 2D is 6% better in terms of wave attenuation as compared to model 2C and 3% better than model A when  $H_i/L$  is 0.02. Their performances became closer to each other as the  $H_i/L$  increased. The probable explanation for this is when the wave was less steep, air bubbles

and vortices can be seen occurring underneath the structure of model 1D. The occurrence of air bubbles and vortices dissipated most of the wave energy during the wave-structure interaction, hence giving a lower  $C_t$  values. This phenomenon was mainly due to the presence of the protruding leg below the structure.

### 4.3 EFFECT OF RELATIVE WIDTH

#### 4.3.1 Experiment 1: Effect of breakwater width and draft

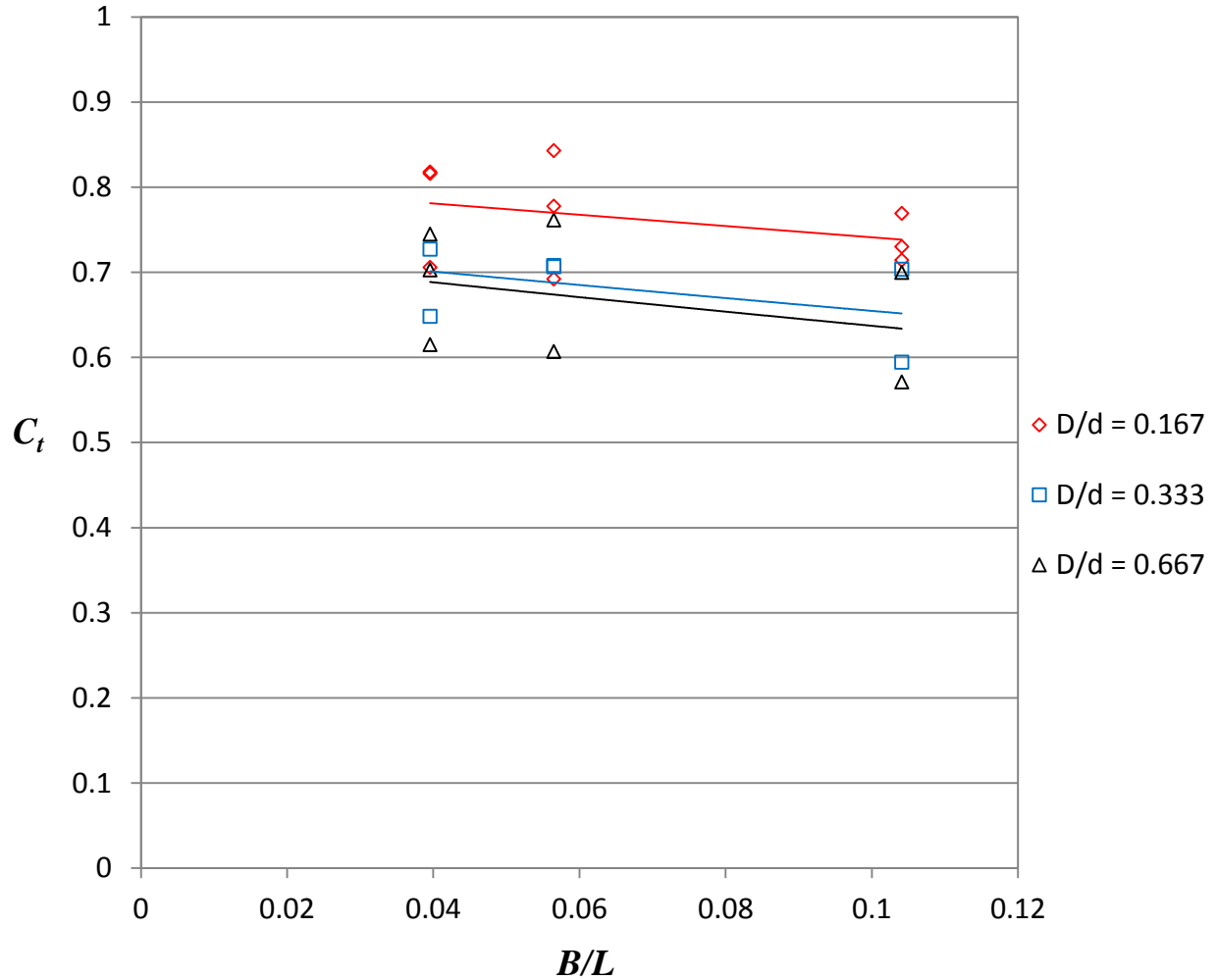
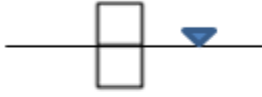
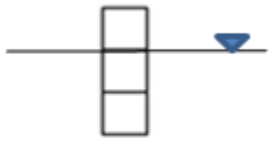
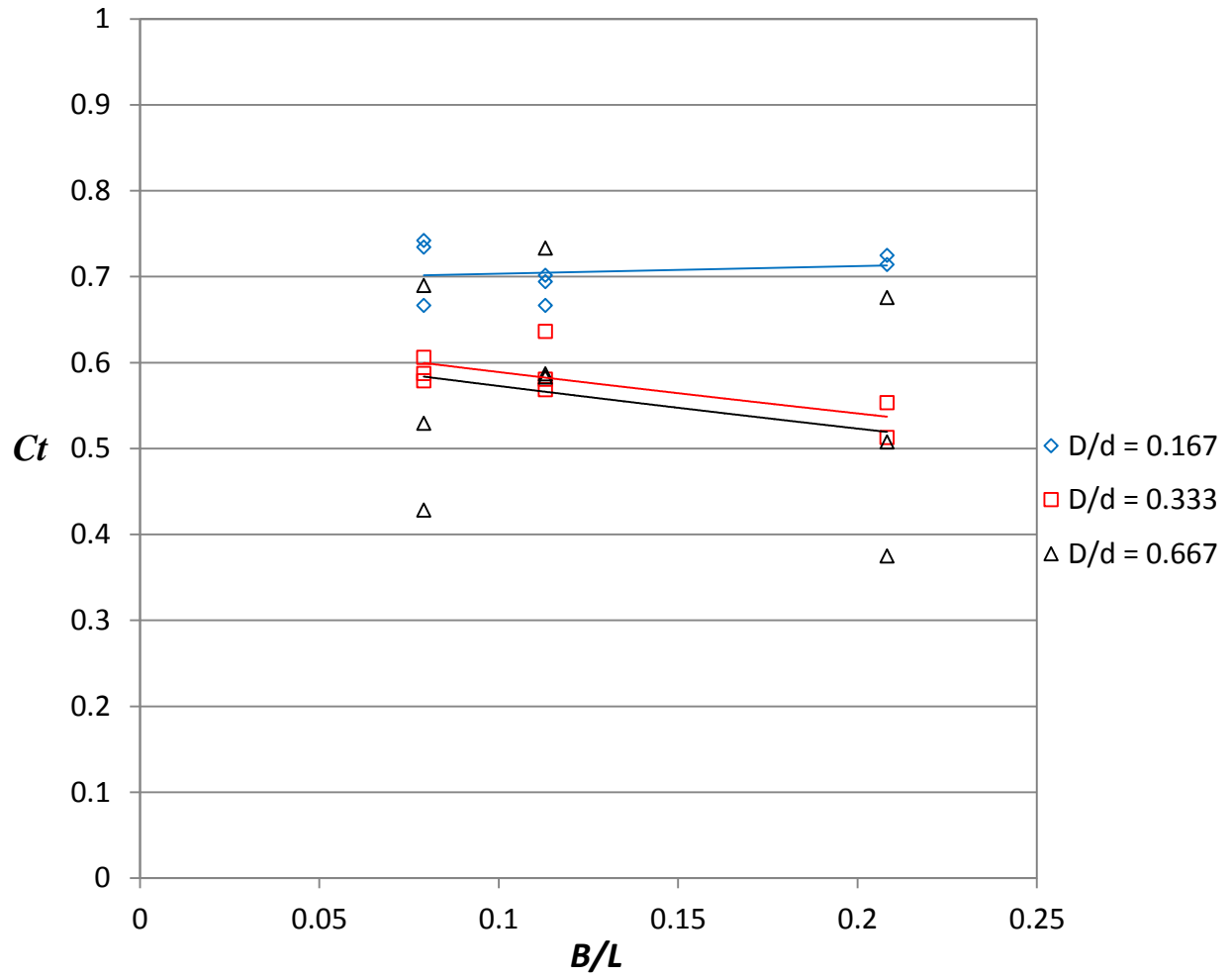


Figure 4.6: Effect of breakwater draft on  $C_t$  of the single column models ( $B/d = 0.333$ )

**Table 4.11: Test parameters for single column models**

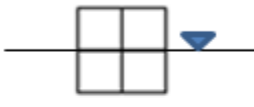
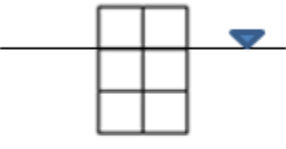
Layout Matrix	1 x 1	2 x 1	3 x 1
Configuration			
$B/d$	0.333	0.333	0.333
$D/d$	0.167	0.333	0.667

**Figure 4.6** demonstrates variation in  $C_t$  values with respect to change in relative width of the structure.  $C_t$  vs  $B/L$  for structures of different drafts are plotted while the width of the structure was being kept constant at 10cm.  $C_t$  values decreased slightly as the relative width values increased. As width is kept constant, it can be said that variation in wave length had little effect on the wave transmission ability of the structure. The plot also represents the effect of relative draft on the wave transmission coefficient. Although variation of  $C_t$  is very small with change in draft of the structure however, maximum values of  $C_t$  ( $C_t > 0.8$ ) were obtained by the model with shallower draft and the model with deeper draft gave relatively lower values ( $C_t < 0.65$ ).



**Figure 4.7: Effect of breakwater draft on  $C_t$  of the double column models ( $B/d = 0.667$ )**

**Table 4.12: Test parameters for double column models**

Layout Matrix	1 x 2	2 x 2	3 x 2
Configuration			
$B/d$	0.667	0.667	0.667
$D/d$	0.167	0.333	0.667

The variation in  $C_t$  values with respect to change in relative width of the structure is being displayed in **Figure 4.7**. With the width of the structure was being kept constant at 20cm,  $C_t$  vs  $B/L$  for structures of different drafts are plotted.  $C_t$  values of model 1 x 2 with  $D/d$  of 0.167 remain almost the same for the relative width values whereas  $C_t$  values for the other two models decreased with the increased of  $B/L$ . Decreasing trend of  $C_t$  with increasing  $B/L$  for the models with higher  $D/d$  values can be explained by the fact that although the width of all the models is same but the deeper draft may play its role for attenuation of shorter waves. The plot also represents the effect of relative draft on the wave transmission coefficient. Relatively higher values of  $C_t$  ( $C_t > 0.7$ ) were obtained by the model with shallower draft and the model with deeper draft gave relatively lower values ( $C_t < 0.5$ ). Moreover,  $C_t$  values are lesser in figure 4.7 as compare to figure 4.6, this shows that wider models can actually attenuate waves more efficiently.

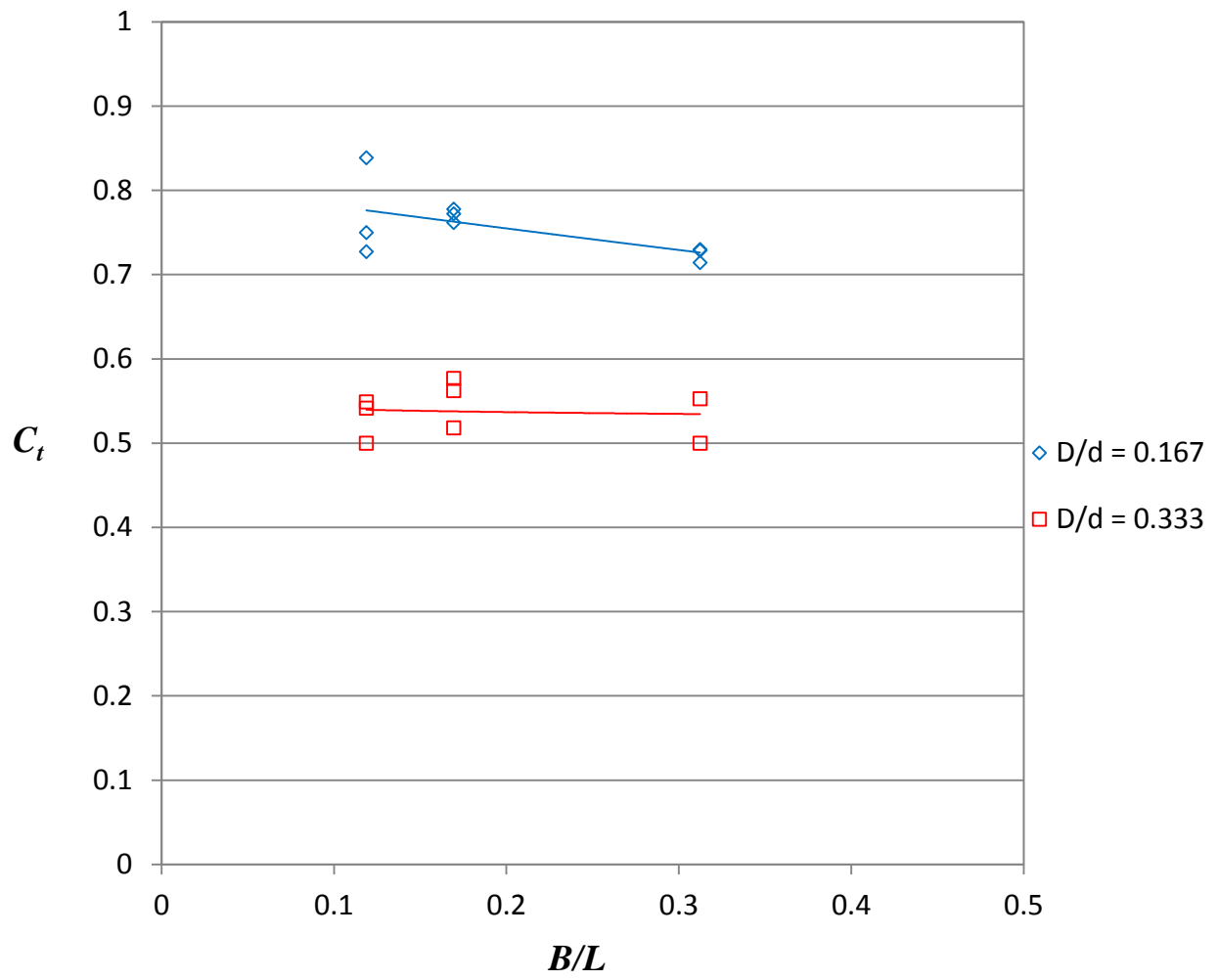
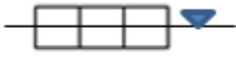
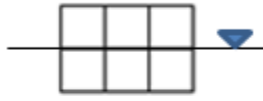
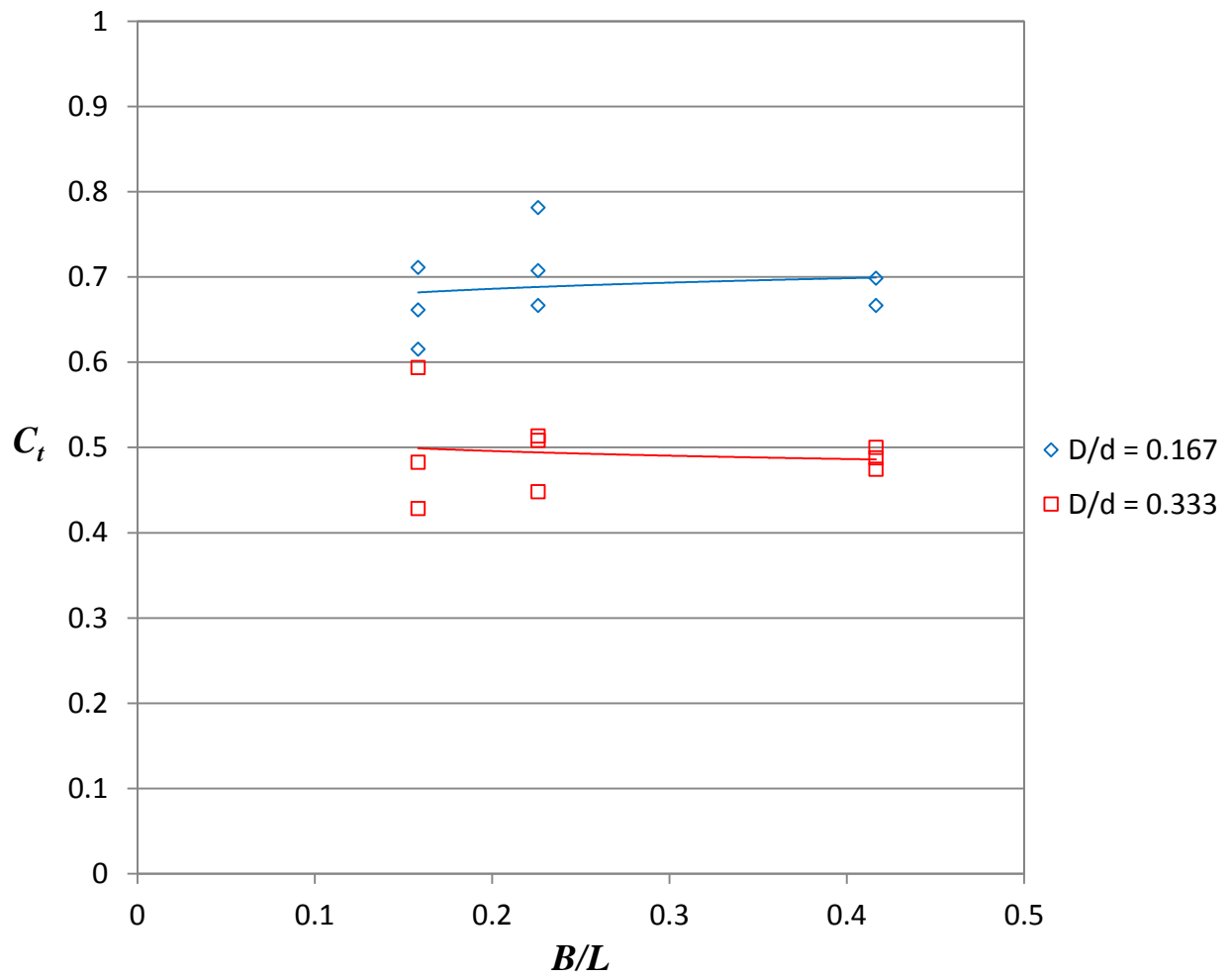


Figure 4.8: Effect of breakwater draft on  $C_t$  of the triple column models ( $B/d = 1.000$ )

**Table 4.13: Test parameters for triple column models**

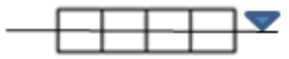
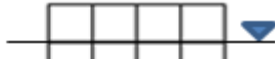
Layout Matrix	1 x 3	2 x 3
Configuration		
$B/d$	1.000	1.000
$D/d$	0.167	0.333

**Figure 4.8** shows variation in  $C_t$  values with respect to change in relative width of the structure.  $C_t$  vs  $B/L$  for structures of different drafts are plotted while maintaining the width of the structure at 30cm.  $C_t$  values for both models remain almost constant throughout the relative width values ranging from 0.1 to 0.3. As width is kept constant, it can be said that variation in wave length had very minimal effect on the wave transmission ability of the structure. The plot also indicates the effect of relative draft on the wave transmission coefficient. The variation of  $C_t$  can be clearly seen with the change in draft of the structure. Maximum values of  $C_t$  ( $C_t > 0.7$ ) were obtained by the model with shallower draft and the model with deeper draft gave relatively lower values ( $C_t < 0.6$ ). Difference of  $C_t$  plots of different  $D/d$  models is very large in **Figure 4.8**, whereas in **Figure 4.6** and **Figure 4.7**, the difference is very small. This shows that effect of draft in enhancing the wave attenuation ability of the structure became very significant for models with larger width.



**Figure 4.9: Effect of breakwater draft on  $C_t$  of the quadruple column models ( $B/d = 1.333$ )**

**Table 4.14: Test parameters for quadruple column models**

Layout Matrix	1 x 4	2 x 4
Configuration		
$B/d$	1.333	1.333
$D/d$	0.167	0.333

**Figure 4.9** displays variation in  $C_t$  values with respect to change in relative width of the structure.  $C_t$  vs  $B/L$  for structures of different drafts are plotted while the width of the structure was being kept constant at 40cm.  $C_t$  values of both models remained almost constant throughout the relative width values ranging from 0.1 to 0.5. This demonstrates that for very wide floating breakwaters, the effect of wavelength on the wave attenuation ability becomes insignificant. The plot also shows the effect of relative draft on the wave transmission coefficient. It can be said that the relative draft of the structure has a significant effect on the  $C_t$  values. Maximum values of  $C_t$  ( $C_t > 0.65$ ) were obtained by the model with shallower draft and the model with deeper draft gave relatively lower values ( $C_t < 0.5$ ). Other than that, the  $C_t$  plots of different  $D/d$  values are also having a huge difference, about 20%, unlike in **Figure 4.5** and **Figure 4.7** which is only about 10 to 15%.

#### 4.3.1.1 Summary

From **Figure 4.6**, **Figure 4.7**, **Figure 4.8** and **Figure 4.9**, we can deduce that  $C_t$  values increased with increase in wavelength for the models with smaller width. However, effect of wavelength on  $C_t$  values was insignificant for wider models. Effect of draft on wave attenuation ability was significant in all the plots. The models with deeper draft performed better in attenuating the waves as compared to the models with shallower draft. This can be explained by the fact that deeper draft does not allow incident waves to underpass the structure hence a larger range of waves can be intercepted by models with higher  $D/d$  values. In addition, this can also be interpreted from the above plots that variation of  $C_t$  values with change in  $D/d$  became more and more prominent as models became wider. From this, we can deduce that smaller variation in draft of a wide model can have a larger effect on its hydrodynamic performance whereas the same amount of variation in draft of a narrow model will have lesser effect on its performance.

### 4.3.2 Experiment 2: Effect of irregular breakwater configuration

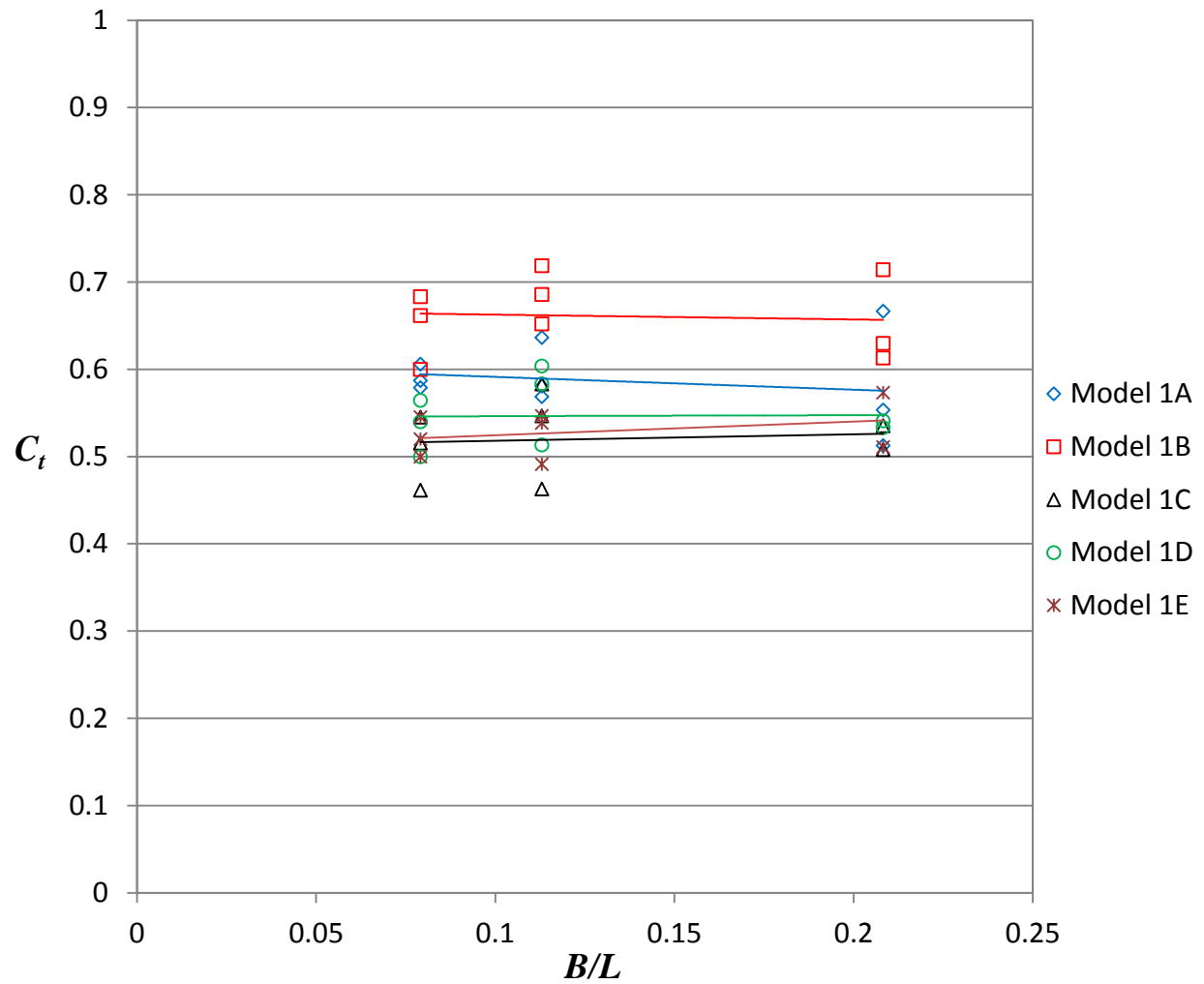
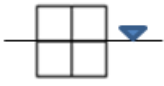
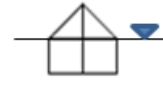
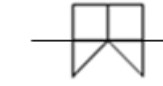
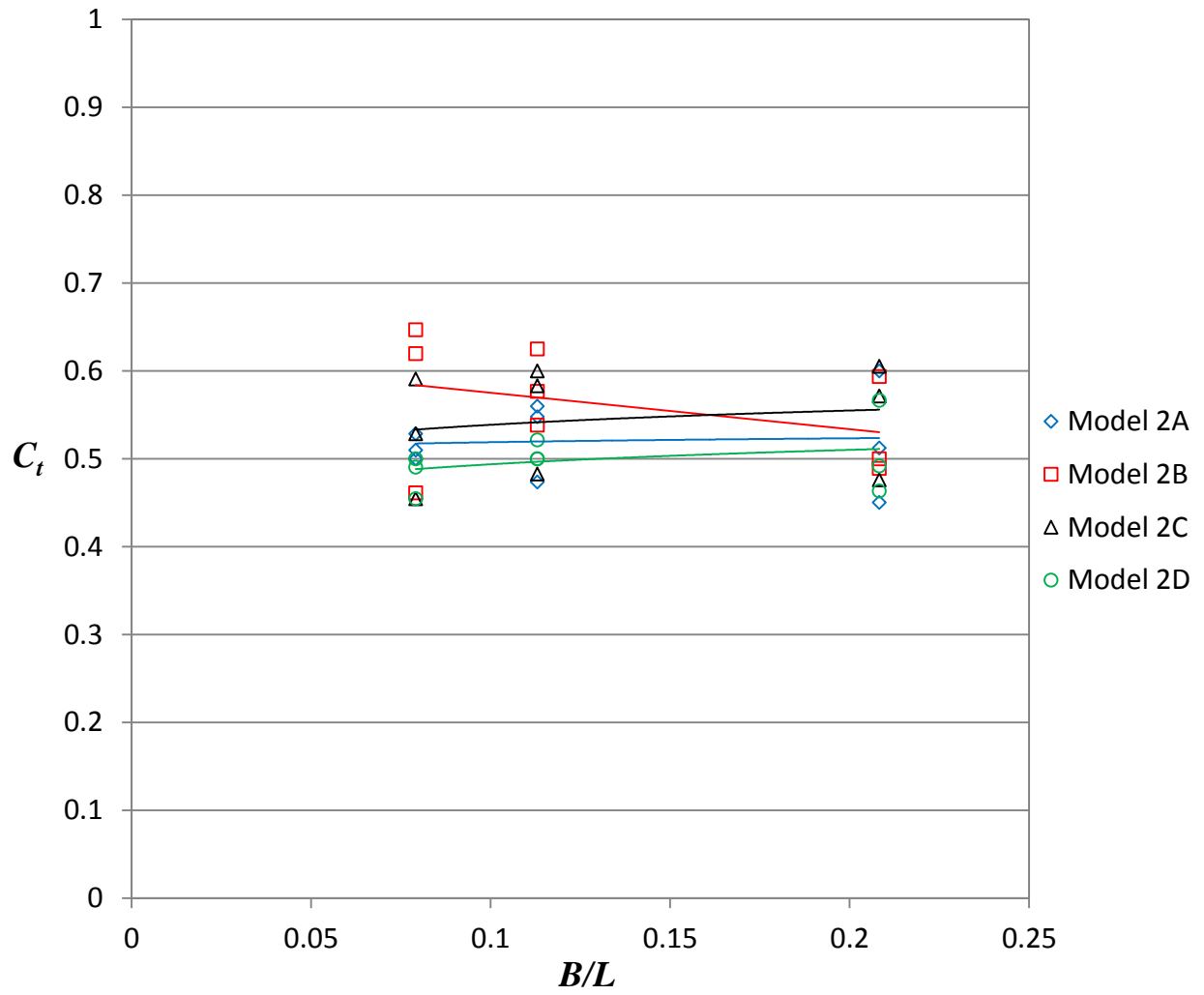


Figure 4.10: Effect of breakwater draft on  $C_t$  of the 2 x 2 matrix models ( $B/d = 0.667$ )

**Table 4.15: Test parameters for 2 x 2 matrix models**

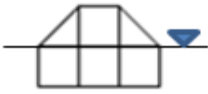
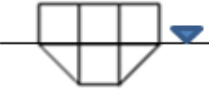
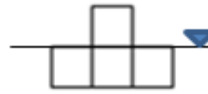
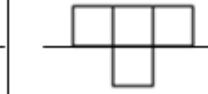
Matrix	1A	1B	1C	1D	1E
Configuration					
$B/d$	0.667	0.667	0.667	0.667	0.667
$D/d$	0.333	0.333	0.333	0.333	0.333

**Figure 4.10** illustrates variation in  $C_t$  values with respect to change in relative width of the structure.  $C_t$  vs  $B/L$  for structures of different configurations are plotted with the width and draft of the structure were being kept constant at 20cm.  $C_t$  values for all models remained constant with increase in  $B/L$ . This shows that relative width does not any significant effect on the wave attenuation ability of these models. Model 1C and model 1E has performed better than all the other models with  $C_t$  values around 0.52. Model 1B had the worst performance with  $C_t$  values ranging up to 0.7. This can be attributed to instable design of the model. All the models except model 1B had wider base whereas model 1B had narrower base.



**Figure 4.11: Effect of breakwater draft on  $C_t$  of the 2 x 3 matrix models ( $B/d = 1.000$ )**

**Table 4.16: Test parameters for 2 x 3 matrix models**

Matrix	2A	2B	2C	2D
Configuration				
$B/d$	1.000	1.000	1.000	1.000
$D/d$	0.333	0.333	0.333	0.333

The variation in  $C_t$  values with respect to change in relative width of the structure is being shown in **Figure 4.11**. It can be seen that  $C_t$  values remain almost constant with increase in  $B/L$ . This shows that there is no significant effect of relative width on wave attenuation ability of these models. Performance of model 2D and 2A was better with  $C_t$  values around 0.5 whereas model 2B and 2C gave slightly higher values of  $C_t$  ranging from 0.5 to 0.65. It is worth mentioning that the difference in performance of all the models is not very large, so further experimentation using wider range of variables can be done to point out the design with the best wave attenuation performance.

## CHAPTER 5

### CONCLUSION AND RECOMMENDATIONS

#### 5.1 CONCLUSION

This research study was to determine the wave transmission characteristics of the rapidly installed modular floating breakwaters in regular waves. The first objective was to evaluate the effects of breakwater width and draft on wave transmission characteristics of the rapidly installed modular floating breakwaters, whereas the second objective was to compare wave attenuation performance of the rapidly installed modular floating breakwaters of different irregular configurations.

The results of the experiment for the first objective in this research study proved that the wave attenuation performance of floating breakwater is better when the draft and also width of the structure increased. However, models with very deep draft actually showed a lot of movement (rolling effect) during the wave-structure interaction. Unfortunately, motion responses and effects of mooring line configurations were not in the scope of this study. Therefore, further studies can be done for these aspects for a better understanding of floating breakwater.

All the models with 2 x 2 matrix and 2 x 3 matrix used in the experiment for second objective had almost the same wave attenuation performance with the exception of the models with hull shape base (Model 1B and Model 2B). The design of those two models should be avoided when designing a floating breakwater since they produced undesirable wave attenuation performance. Nevertheless, detailed study should be further carried out with wider range of variables to find out the floating breakwater configuration that gives the most desirable wave attenuation performance.

It is worth mentioning that models with almost the same wave attenuation performances can have different applications in different site conditions. In the real world problems, every site has its own conditions and performance requirements; hence decision cannot be made based only on the experimental results. Engineering judgement also plays an important role in decision making.

## 5.2 RECOMMENDATIONS

The rapidly installed floating breakwaters developed in this study have met the initial design objectives – flexibility, easy installation and reasonably good wave attenuation performance. However, some recommended activities can be taken into consideration for future research in order to fully understand the behavior of floating breakwater.

- Wave probes should be used to increase the accuracy of the results.
- Motion responses and effects of mooring line configurations should be considered for better understanding of floating breakwater.
- Breakwater models should be subjected to random and oblique waves in order to stimulate real marine environment and also to determine the resonance of the structure.
- Larger scale experimentation should be done to improve the scaling effects.
- Numerical modelling should be carried out for the validation of experimental results.

## REFERENCES

- Blenkinsopp, C. E. and J. R. Chaplin (2011). *Void fraction measurements and scale effects in breaking waves in freshwater and seawater*. *Coastal Engineering* 58(5): 417-428.
- Briggs, M. J. (2001). *Performance Characteristics of a Rapidly Installed Breakwater System*. U.S. Army Engineer Research and Development Center.
- Chakrabarti, S. K. (1999). Wave interaction with an upright breakwater structure. *Ocean Engineering*, 26(10), 1003-1021.
- Dillon Consulting Limited. (2013). Breakwater Improvements. *Hamilton West Harbour Shoreline and Breakwater Class Environmental Assessment: Environmental Study Report*. 70-85.
- Dobling, M. (2003). *Rapidly Installed Breakwater (RIB) Systems*. University of Wisconsin-Madison.
- Dong, G. H., Zheng, Y. N., Li, Y. C., Teng, B., Guan, C. T., & Lin, D. F. (2008). Experiments on wave transmission coefficients of floating breakwaters. *Ocean Engineering*, 35(8–9), 931-938.
- Fousert, M. W., (2006). Floating breakwater: A theoretical study of hydrodynamic performance of a attenuating system. Faculty of Civil Engineering and Geosciences, Delft University of Tehcnology.
- Gesraha, M. R. (2006). Analysis of shaped floating breakwater in oblique waves: I. Impervious rigid wave boards. *Applied Ocean Research*, 28(5), 327-338.
- He, F., Huang, Z., & Wing-Keung Law, A. (2012). Hydrodynamic performance of a rectangular floating breakwater with and without pneumatic chambers: An experimental study. *Ocean Engineering*, 51, 16-27.
- Heller, V. 2011. Scale effects in physical hydraulic engineering models. *Journal of Hydraulic Research* 49(3), pp. 293-306.
- Hughes, S. A., 1993. *Physical Models and Laboratory Techniques in Coastal Engineering*. Advanced Series on Ocean Engineering, World Scientific, Singapore, Vol.7. ISBN:981-02-1541-X.
- Ji, C.-Y., Chen, X., Cui, J., Yuan, Z.-M., & Incecik, A. (2015). Experimental study of a new type of floating breakwater. *Ocean Engineering*, 105, 295-303.

- Kumar, P. S. (2008). *Studies on a Class of Vertical Submerged and Floating Breakwaters in a Two-Layer Fluid*. Indian Institute of Technology.
- Li, J., Wang, Z., & Liu, S. (2012). Experimental study of interactions between multi-directional focused wave and vertical circular cylinder, Part I: Wave run-up. *Coastal Engineering*, 64, 151-160.
- McCartney, B., (1985). Floating Breakwater design. *Journal of Waterway, Port, Coastal, and Ocean Engineering*, 111(2), pp.304-318.
- Mani, J. (1991). Design of Y-Frame Floating Breakwater. *Ocean Engineering*, 117(2), 105–119.
- Mulvihill, E. L., Francisco, C. A., Glad, J. B., & Kaster, K. B. (1980). Biological impacts of minor shoreline structures on the coastal environment: state-of-the-art review. Vol. I, 156 pp. Vol. II *FWS/OBS* (- ed.).
- Pfister, M. and H. Chanson (2012). *Scale effects in physical hydraulic engineering models* By VALENTIN HELLER, *Journal of Hydraulic Research*, Vol. 49, No. 3 (2011), pp. 293–306. *Journal of Hydraulic Research* 50(2): 244-246.
- Sannasiraj, S. A., Sundar, V., & Sundaravadivelu, R. (1998). Mooring forces and motion responses of pontoon-type floating breakwaters. *Ocean Engineering*, 25(1), 27-48.
- Teh, H. M., & Mohammed, N. I. (2012). *Wave interactions with a floating breakwater*. Paper presented at the Humanities, Science and Engineering (CHUSER), 2012 IEEE Colloquium on.
- Waveblocks. (2014). *Open Innovation Challenge (OIC)*. 35<sup>th</sup> Science & Engineering Design Exhibition (SEDEX) of Universiti Teknologi PETRONAS (UTP).
- Wavebrake. *Home*. Retrieved 31<sup>st</sup> October 2015 from: <http://www.wavebrake.com/index.html>
- WaveEater. *Home*. Retrieved 31<sup>st</sup> October 2015 from: <http://waveeater.com/>
- WhisprWave®. *Wave Attenuators*. Retrieved 31<sup>st</sup> October 2015 from: <http://www.whisprwave.com/products/wave-attenuators/>
- Williams, A. N., & Abul-Azm, A. G. (1997). Dual pontoon floating breakwater. *Ocean Engineering*, 24(5), 465-478.